

Torsional Splittings and Assignments of the Doppler-Limited Spectrum of Ethane in the C-H Stretching Region*

A. S. Pine** and W. J. Lafferty**

National Bureau of Standards, Washington, DC 20234

November 18, 1981

The Doppler-limited absorption spectrum of the C-H stretching region of ethane has been recorded at $T \approx 119$ K with a tunable difference-frequency laser spectrometer. The strong torsional hot band structure at room temperature is eliminated at 119 K, and the enhanced resolution from the Doppler width reduction allows us to observe small torsional splittings. The two fundamentals in the region, ν_7 , a perpendicular band and, ν_5 , a parallel band have been essentially completely assigned as have a large number of transitions in the parallel component of the $\nu_8 + \nu_{11}$ combination band. A number of perturbations of both global and local nature have been observed. The complete spectrum and a listing of transition wavenumbers, intensities and assignments are presented here to facilitate identification and quantitative analysis of ethane in a variety of monitoring applications. Precise ground state rotational constants have been determined from combination differences.

Key words: C-H stretching region; difference- frequency laser; Doppler-limited resolution; ethane; ground state constants; infrared spectrum; low temperature spectrum; torsional splittings.

1. Introduction

Although ethane is the simplest hydrocarbon containing a saturated carbon-carbon bond and has very high symmetry (D_{3d}), the extremely dense and complex rotational fine structure of its infrared bands has defied complete resolution until recent advances in Doppler-limited tunable laser and Fourier transform instrumentation. Previously, high-quality grating spectra of the C-H stretching region at 0.025 cm^{-1} resolution permitted Cole, Lafferty and Thibault [1]¹ to partially assign the rotational transitions of the ν_7 perpendicular band. More recently Cole, Cross, Cugley and Heise [2] deconvolved similar grating data to $\sim 0.015\text{ cm}^{-1}$ to observe somewhat more structure in this same band. We present here the Doppler-limited absorption spectrum of the infrared active C-H stretches of ethane recorded at $T \approx 119$ K (Doppler FWHM = 0.0043 cm^{-1}) with a tunable difference-frequency laser spectrometer. Both fundamentals, ν_7 centered at 2985.39 cm^{-1} and the parallel band ν_5 at 2895.67 cm^{-1} , have been fully resolved

and assigned, and much of the $\nu_8 + \nu_{11}$ combination band has been identified.

The principal complications in the infrared spectrum of C_2H_6 arise from the relative torsional motion of the two methyl groups about the saturated C-C bond [3]. The moderate potential barrier (of $\sim 1024\text{ cm}^{-1}$) to free internal rotation leads to a low frequency torsional mode ν_4 at $\sim 290\text{ cm}^{-1}$ as determined by a number of calorimetric [4,5] and spectroscopic [6,7] techniques. This mode is highly excited at room temperature giving rise to "hot bands" associated with each normal band originating in the ground vibrational state. These hot bands are effectively suppressed in the present study by maintaining the ethane sample at the lowest possible temperature above the vapor condensation point. Overtones and combination states of this low frequency torsional mode are also in Fermi or Coriolis resonance with virtually all the higher vibrations of the molecule, causing severe perturbations whose complexity increases dramatically with the wavenumber of the other bands because of the increasing number of possible combinations.

Tunneling through the torsional potential barrier creates a further doubling of the energy levels of the molecules which may be manifest as small splittings in the rovibrational transitions as discussed by Susskind [8]. However, for nontorsional modes, such as those studied here, the barrier and, hence, the torsional split-

*The experimental portion of this work was performed while the author was with Lincoln Laboratory of the Massachusetts Institute of Technology under NSF Contract #NSF/ASRA/DAR 78-24562. A preliminary account of this work appears in the NSF Final Report entitled "Tunable Laser Survey of Molecular Air Pollutants: Doppler-Limited Spectra of the C-H Stretching Bands of Formaldehyde, Ethylene, Ethane and Allene," January 1980.

**Molecular Spectroscopy Division, National Measurement Laboratory.

¹Figures in brackets indicate literature references at the end of this paper.

tings are not expected to vary significantly from the ground state. Thus the splittings for nontorsional infrared transitions, which arise from the *difference* in the splittings of the upper and lower vibrational levels [8], are expected to be unresolvable, even at the Doppler limit. Nevertheless the resonant interactions with torsional overtones and combinations, mentioned above, induce variations in the barrier giving rise to observable torsional splittings in the present work. Some of these are illustrated in figure 1 for the region around RQ_5 of the ν_7 band, as brought out by the resolution enhancement and spectrum simplification resulting from lowering the ethane temperature. The torsional doublets of the $RR_2(7)$ and $RR_3(4)$ lines and the interleaved RQ_5 subbranch are unambiguously characterized by their nuclear spin statistical weight intensity ratios calculated by Wilson [9].

The first observation of torsional splitting in ethane was made in diode laser spectra of the ν_9 band by Patterson, Flicker, McDowell and Nereson [10]. These splittings also arise from perturbations, induced by a resonance with $3\nu_4$; but since that is the only possible

resonance with ν_9 , that band is more amenable to analysis than the complex C-H stretching bands. Two detailed studies of the ν_9 band are now in progress [11,12]; both are based on Doppler-limited diode laser spectra of the Q branches and comprehensive, precision Fourier transform interferometer data. In the present study of the C-H stretches, the torsional splittings exhibit many interesting patterns indicative of a variety of interactions and perturbing states.

The complex low temperature Doppler-limited spectrum of ethane between 3051 and 2862 cm^{-1} is given in this report along with a listing of transition wavenumbers, intensities and assignments. We also discuss the assignment procedure and the more interesting spectral features associated with the perturbations, torsional splittings and combination bands. A precise set of ground state rotational constants obtained from combination differences is given since microwave data do not exist for this nonpolar molecule. These definitive spectra are truly characteristic of the molecule without instrumental distortion since the laser linewidth ($\sim 0.0003 \text{ cm}^{-1}$) is much narrower than the Doppler width. Hence, the spectral patterns should be useful for the identification and quantitative analysis of ethane for a number of practical applications. For example, ethane is a principal constituent of natural gas (0 to 20% with $\sim 7\%$ average) and can be used for labelling sources, detecting leaks and monitoring pipeline transmission and LNG carriers [13]; it is one of the major hydrocarbon emissions in automobile exhausts and can interfere with the measurement of more toxic components [14]; and it has been observed in the atmosphere of several outer planets [15] with significance to extraterrestrial organic chemistry.

2. Experimental Considerations

The high resolution ethane spectra reported here were recorded with a tunable difference-frequency laser spectrometer developed at MIT Lincoln Laboratory for obtaining precise and comprehensive Doppler-limited vapor-phase spectra in the 2.2 to 4.2 μm region. The instrument is based on the nonlinear optical down-conversion of CW visible single-mode argon ion and tunable dye lasers in a LiNbO_3 mixing crystal. The basic operating characteristics of the system [16] along with techniques of drift compensation [17], stabilization and automated data processing [18] and linear scan control [19] have been detailed elsewhere, so we will discuss here only those features pertinent to the present investigation.

Since the C-H stretching bands of ethane are quite extensive (covering $\sim 200 \text{ cm}^{-1}$), the difference-frequency system was operated in a broad survey, rapid scan mode. The absorption spectra were recorded in continuously

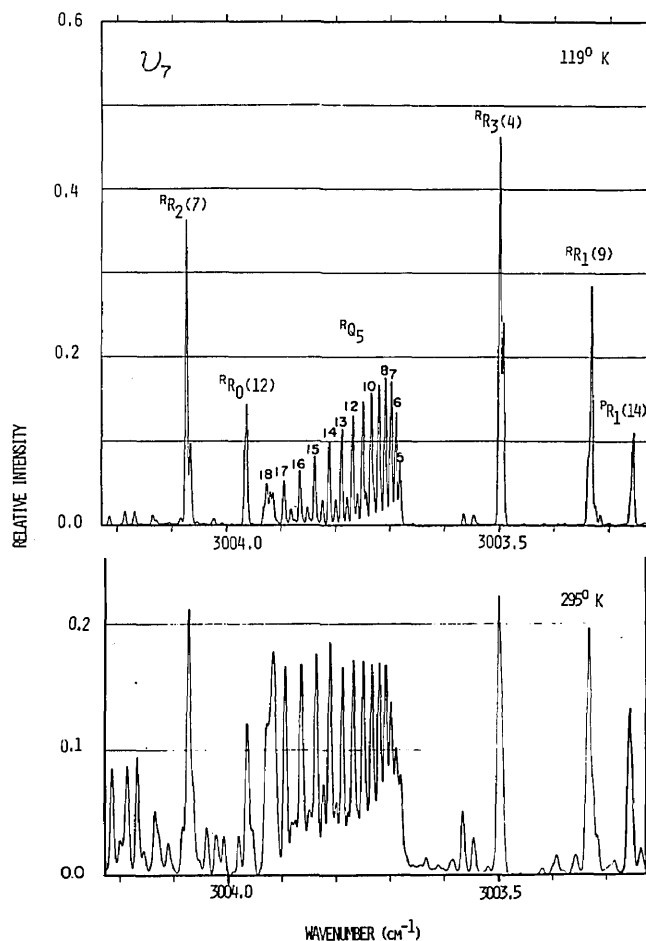


FIGURE 1. Comparison of the ethane spectrum in the region of the RQ_5 subbranch of the ν_7 band for temperatures of 119 K and 295 K.

scanned 3.75 cm^{-1} segments overlapped at intervals of 3 cm^{-1} . The scan rate was $0.0125\text{ cm}^{-1}/\text{s}$ or 375 MHz/s so each segment was scanned in 5 minutes. The post-detection time constant was 40 ms (corresponding to 5×10^{-4} or 15 MHz) which was short enough to allow full response to the sharp Doppler-broadened lines (FWHM = 128 MHz for C_2H_6 at $T \approx 119\text{ K}$) but long enough for good signal-to-noise ratio of ~ 500 . The transmission traces were digitized at a 20 Hz rate (6000 points per segment, $6.25 \times 10^{-4}\text{ cm}^{-1}$ per point) for data storage and subsequent numerical processing. The instrumental width, due primarily to the dye laser free-running jitter, was about 10 MHz FWHM. Thus the effect of instrumental broadening is negligible since convolution of the Gaussian profiles of the Doppler and laser distributions results in the widths adding in quadrature.

The ethane spectra were recorded over a period of 2 days. Each day's run was calibrated against CH_4 reference lines from the Fourier transform interferometer data of Tarrago *et al.* [20]. The first day's run was interpolated between the R(3) and P(7) manifolds of the ν_3 band of CH_4 while that of the second day between P(7) and P(15) using a 5 cm confocal Fabry-Perot interferometer with a free spectral range of $0.050027(1)\text{ cm}^{-1}$. The interorder spacing of this scan calibration interferometer can be measured to a precision of $\pm 2 \times 10^{-7}\text{ cm}^{-1}$ over a 100 cm^{-1} interval, but it exhibits a small frequency dispersion and overnight thermal shifts which must be checked during extended runs. The determination of the spectral line wavenumbers for these rapid survey scans was made to a relative precision of $\sim \pm 4 \times 10^{-4}\text{ cm}^{-1}$ which was slightly better than the least reading for the digitizing grid. The absolute accuracy of the wavenumbers may be slightly worse due to uncertainties in the reference line standards.

In order to obtain line strength information from the transmission traces, one must account for Beer's law, $\alpha(\omega) = (\rho L)^{-1} \ln(B(\omega)/S(\omega))$. Here $\alpha(\omega)$ is the absorption coefficient in units of $(\rho L)^{-1}$ where ρ is the sample density and L is the cell length; $S(\omega)$ is the transmission and $B(\omega)$ is the empty cell baseline. In this case the baseline was entered manually on a coarse grid (0.125 cm^{-1}) since it was not practical to evacuate the cold cell and refill for each trace. Also our automatic baseline interpolation routine, which keys on the background between lines, did not work reliably for ethane since the spectrum was so dense. The manual baseline estimation is only adequate to $\sim \pm 1$ percent because of strong channeling of the spectra from the cold cell windows. The baseline uncertainties dominate the relative line strength errors since the actual transmission spectra are reproducible to $\approx \pm 0.2$ percent. In addition, absolute intensities depend on measurement accuracy of the cell length ($29.4 \pm 0.1\text{ cm}$), the fill pressure ($225 \pm 4\text{ m Torr}$ at $T = 295 \pm 1$

K), the sample temperature (held at $T = 119 \pm 3\text{ K}$) and, to a lesser extent, on sample purity. Here we used natural isotopic ethane of research grade from Matheson with a quoted purity of 99.96 percent; it exhibited no trace of methane or other simple hydrocarbons in the spectrum. In the atlas, corrections are made for the isotopic abundance of $^{12}\text{C}_2\text{H}_6$.

The sample cold cell was a copper tube with thinned end sections for stress-free epoxy mounting of ZnSe windows required because of differential thermal contraction. Copper cooling coils were soldered to the tube and an evacuable stainless steel jacket with CaF_2 windows provided thermal isolation. The cell was cooled by manually controlling the flow of He gas through a liquid N_2 heat exchanger and then through the cell coils. The temperature was measured with a single platinum resistance thermometer imbedded in the copper cell wall. The uniformity of the temperature is expected to be better than the manually controlled temperature setting which dominates the absolute intensity errors ($\sim \pm 3\%$ for low J and K).

3. Spectral Features

The fundamentals, ν_5 and ν_7 , are examples of parallel and perpendicular bands whose assignment, as is customary, is based on selection rules, "missing lines" and consistent ground state combination differences. Where observed, the torsional doublets provide a definitive confirmation of the K and some J assignments because of their distinctive intensity ratios for particular rotational quantum numbers. The nuclear spin statistical weights for these doublets derived by Wilson [9] yield the intensity ratios of 4:1 for K not a multiple of 3; 2:1 for K a multiple of 3 but not 0; and for $K = 0$ a ratio of 3:1 for J even and 5:3 for J odd. These ratios are illustrated in figure 1 for $K = 2, 3$ and 5 levels of ν_7 and in figure 2 for the $K = 0, 2$ and 4 cases in the P(6) and P(7) manifolds of ν_5 . Each torsional component is labelled in the atlas according to the ground state symmetry species of the permutation-inversion group G_{36}^+ for ethane-like molecules exhibiting internal rotation as discussed by Hougen [21].

Though the assignments for the fundamentals are firm and rather complete, a number of severe perturbations are observed due to accidental resonant crossings of energy levels. However, for both ν_5 and ν_7 the initial K subband lines at $J = K$ appear regular and undisturbed. This implies that both bands are affected by X-Y Coriolis interactions since the matrix elements governing such a resonance are proportional to $[J(J+1) - K(K+1)]^{1/2}$. In most cases the effect of such a perturbation is to change the effective B values of individual subbands but to leave the K structure unaffected. However, for the

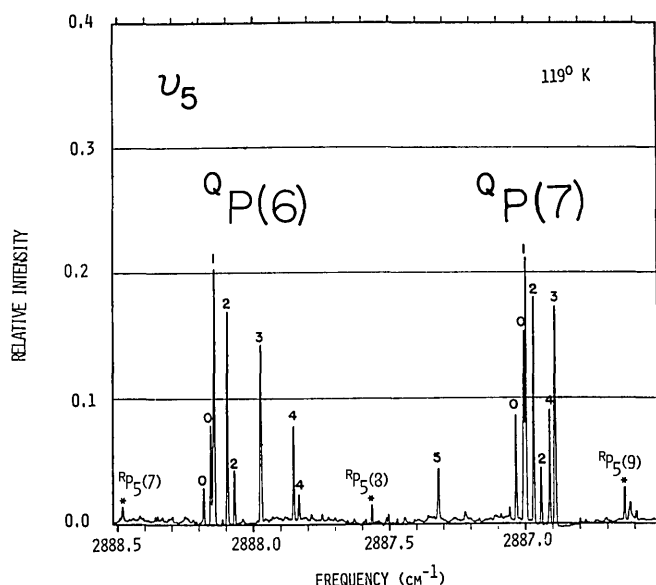


FIGURE 2. Spectrum of C_2H_6 near the P(6) and P(7) manifolds of the ν_5 band at $T = 119$ K. Perturbation-induced lines are labelled with an *.

very close resonances observed in some of the subbands here, the perturbations are severe enough that they cannot be fit using a standard power series expansion. In ν_7 such a resonance is dramatically exhibited by the RQ_5 subbranch shown in figure 1. This subbranch is much more spread out than lower RQ_K subbranches and is degraded in opposite direction to the higher RQ_K subbranches; it also shows an abrupt head and gap above $J = 18$. In addition, there are numerous smaller local perturbations, one of which, shown in figure 3, occurs in the

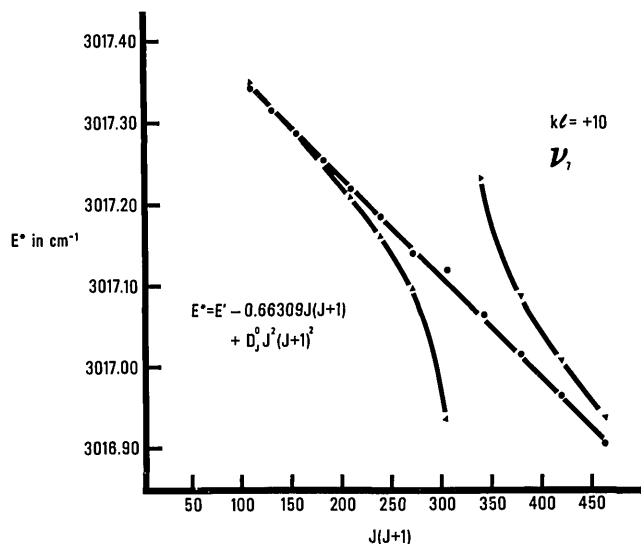


FIGURE 3. Torsional splittings in the $K' = 10$, $\Delta K = +1$ subband of ν_7 . The dots represent the stronger $A_{1s} - A_{2s}$ symmetry components and the triangles represent the weaker $E_{3s} - E_{4s}$ symmetry components.

$K = 10$, $\Delta K = +1$ subband, manifest in a rapid increase in the torsional splitting as a function of J to a value ~ 0.1 cm^{-1} at $J' = 17$, above which it suddenly reverses sign and decreases again to higher J' . In some subbands of ν_7 the torsional splitting is constant or a monotonic function of $J(J+1)$ and in others it appears to be irregular.

On the other hand, perturbations in ν_5 appear to be dominated by a strong resonance near the $K = 5$ energy level stack. The effect of this resonance is to degrade the $K = 5$ subband to lower frequency while the others are degraded to higher frequency as shown in figure 4. Despite the degradation, the subband "origins" at $J = K$ fall on a relatively unperturbed straight line, as seen in figure 4, implicating the X-Y Coriolis interaction. From

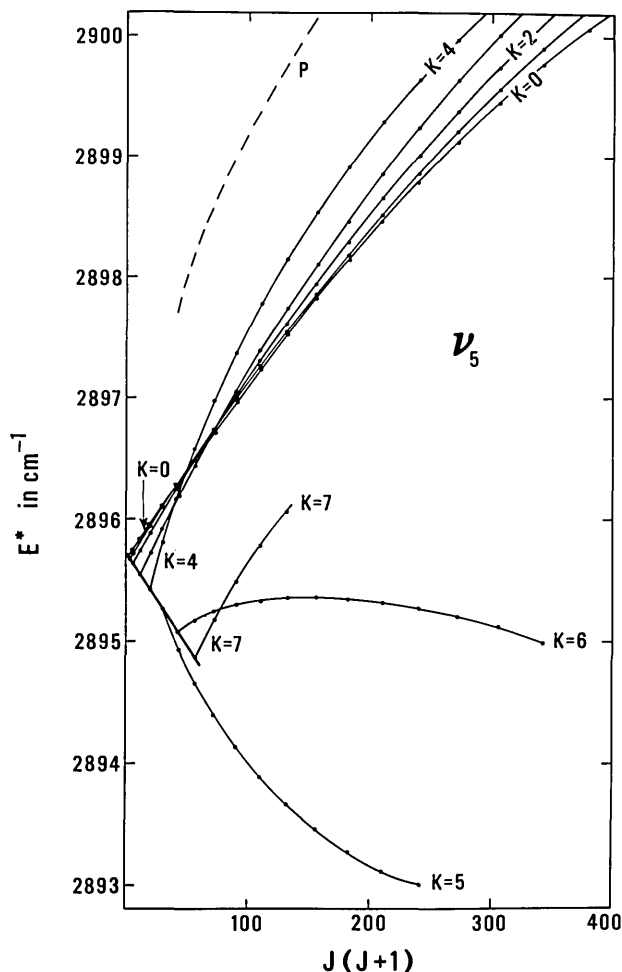


FIGURE 4. Reduced energy for the stronger torsional components of the K subbands of ν_5 . The dashed line represents the $K = 6$ subband of an E_u vibration perturbing $K = 5$ of ν_5 and observed by resonant mixing. Here $E^* = \nu_5(J'K, J''K'') + B_5 J''(j'' + 1) - B_5^* J'(J' + 1)$ where $\nu_5(J'K', J''K'')$ are the transition wavenumbers for the band and $B_5^* = 0.6624$ cm^{-1} is chosen to adjust the scale of the plot.

the a_{2u} symmetry of ν_5 and the E_g species for the vibrational operator of the X-Y Coriolis coupling, we can conclude that the perturbing vibration has E_u symmetry. The resonance mixing is strong enough near the crossover that the perturbing levels accompanying the $K = 4$ and 5 subbands borrow sufficient intensity to be observed in the spectrum. The levels perturbing $K = 5$ are positioned along the dashed curve, labelled P in figure 4, and a few of the corresponding perturbation-induced transitions are shown in figure 2, labelled with an asterisk. We believe that these perturbing levels belong to the $K = 6$ subband of the resonant state because of the $\Delta K = \pm 1$ requirement for the X-Y Coriolis interaction and the fact that the $J = K = 5$ level of ν_5 is unperturbed. The K assignments for the perturbing subbands must be regarded as tentative since we have so few series, but they are consistent with the intensity ratios of their torsional doublets which have splittings comparable to those in ν_5 .

The perturbation-induced torsional splittings take the interesting form shown in figure 5. For the odd K subbands the $J = K$ transitions are not observably split, but at higher J the splitting increases regularly, to as much as $\sim 0.1 \text{ cm}^{-1}$ in some cases. Even for the most perturbed subband, $K = 5$, the doublet of the $J = 5$ transition is not resolved while $J = 6$ is. In the even K subbands however, the $J = K$ transitions are all split by $\sim 0.02 \text{ cm}^{-1}$ and, except for $K = 6$, the splittings increase slowly with J . For $K = 6$ the splittings decrease with J , become unresolved at about $J = 14$ and are resolved again at higher J with the splittings reversed. We currently have no consistent model for this striking behavior of the torsional splittings in ν_5 . It is clear however, that recognizing the presence of torsional doubling was the key to assigning ν_5 which was missing in prior studies [1,2].

The combination bands present a somewhat more difficult situation to analyze. First there are ambiguities in

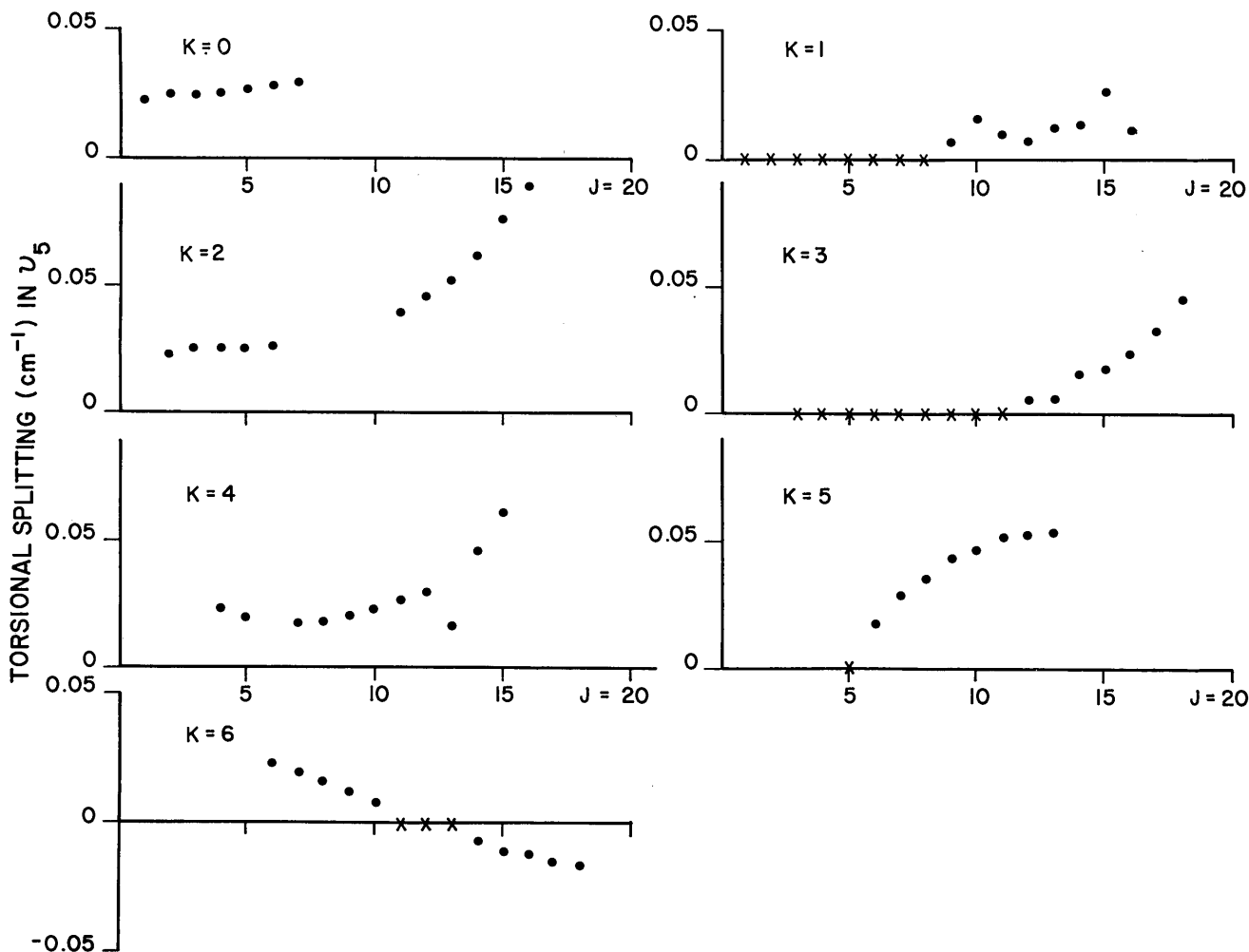


FIGURE 5. Torsional splittings in the ν_5 band of C_2H_6 for $0 \leq K \leq 6$. Here X represents unresolved doublets.

the vibrational sublevel symmetries for the $\nu_8 + \nu_{11}$ combination band since there are several components possible ($e_u \times e_g = A_{1u} + A_{2u} + E_u$). The E_u component of $\nu_8 + \nu_{11}$ should result in a perpendicular band with an effective $\xi_+ = -(\xi_8 + \xi_{11}) \simeq +0.71$ from the data of Nakagawa and Shimanouchi [22], leading to P, R, Q_K subbranches spaced by $\sim 7.8 \text{ cm}^{-1}$. We see no direct evidence for such a band in our spectrum. On the other hand, we see at least two moderately strong parallel bands belonging to the A_u components. To first order only the A_{2u} mode should be infrared active, but the normally inactive A_{1u} mode may borrow intensity from A_{2u} via a Z-type Coriolis interaction proportional to $H_{12} = -AK\xi_-$, where $\xi_- = |\xi_8 - \xi_{11}|$, as discussed by Hougen [23]. The appearance of the $A_1 - A_2$ band also depends on the separation, ΔE , between these two states. In the uncoupled limit where either ΔE is large or H_{12} is small, the mixing is negligible and only transitions to the ordinary A_{2u} parallel band would be observed. If $\Delta E = 0$ the mixing will be complete and the resulting infrared band will have the appearance of a perpendicular band (with parallel band intensity patterns [24]) with a Coriolis constant ξ_- . Intermediate cases require a more detailed calculation. The two modes can be distinguished by the presence of a $K = 0$ subband allowed for A_{2u} and forbidden for A_{1u} since the Coriolis coupling is proportional to K .

A number of parallel-type subbands were assigned in this region by first identifying strong series in the R branch with estimated J and K and calculating the Q and P lines using the precise ground state combination differences obtained from the fundamental bands. If the series matches observed lines to within $\sim 0.0005 \text{ cm}^{-1}$ and the intensities are consistent, then one can be quite confident of the J assignment. The K assignment is less certain because the combination differences are not strongly K dependent. However again, where torsional splittings are observed ($K = 0$ and 3 in this instance) the K assignments are verified by the doublet intensity ratios. The other subbands were assigned K values according to the missing lines resulting from $J \geq K$. In the P and R branches, the lower J transitions are weak and often obscured and overlapped by stronger series. For the Q branch of a parallel band, the lowest J line is strongest, so the Q branches were most useful in establishing the K numbering of the series. One subband has a very small value of $B' - B''$ and its Q subbranch, falling at $2958.0863 \text{ cm}^{-1}$, is not resolved. This subband is tentatively believed to involve $K = 2$ transitions with an uncertainty of ± 1 in K . The prominent feature in the spectrum at about 2953.8 cm^{-1} consists of Q subbranches ranging from $K = 2$ to 6. The lower K subbands have origins both above and below this feature; namely $K = 0$ at $2955.6699(2) \text{ cm}^{-1}$, $K = 1$ at

$2956.1196(4) \text{ cm}^{-1}$ and $2951.9962(2) \text{ cm}^{-1}$ and $K = 2$ at $2958.0866(8) \text{ cm}^{-1}$.

Although the majority of lines occurring in the combination band region have been assigned, their subbands are badly perturbed and many strong series remain unidentified. The ν_8 and ν_{11} band is expected to have both Fermi and Coriolis interactions with the fundamentals and with other higher order overtones and combinations. Also Hougen [25] has pointed out the possibility of an interaction between the A_{1u} component and the totally symmetric a_{1g} C-H stretching mode, ν_1 , in ethane-like molecules with an intermediate barrier. This interaction, strictly forbidden for rigid D_{3d} molecules, is permitted during the torsional tunneling motion. It is of course expected to be weak in ethane but the near degeneracy with the Raman-active ν_1 mode at 2953.7 cm^{-1} as determined by Lepard, Shaw and Welsh [26] may account for some of the observed anomalies in this band.

4. Ground State Constants

Since ethane is nonpolar, no microwave data are available for the ground state rotational constants. Thus we have calculated the rotational constants from the large number of ground state combination differences (CDs) collected during the course of the assignment of the C-H stretching bands. We have restricted the CDs used in obtaining the constants to those obtained from the two fundamentals, ν_5 and ν_7 , since the lines from these bands are stronger, more precisely measured than those in the combination band, and the assignment is firm in these bands. In calculating CDs from transitions which were split into torsional components, the lines were assigned the ground state symmetry of Hougen [21] according to the observed intensity ratios, and differences were taken between components of the same symmetry. A number of lines were unsplit and, if these lines were sharp, CDs between them were also included in the fit. Lines for which the torsional splitting was only poorly resolved were not included in the fit.

The ground state constants of a prolate symmetric top molecule are defined by the usual term value equation:

$$F(J, K) = (A_0 - B_0)K^2 + B_0 J(J + 1) - D_J^J J^2(J + 1)^2 - D_J^K K^2(J + 1) - D_K^K K^4.$$

No "forbidden" transitions with $|\Delta K| > 1$ were observed in the spectrum so only the coefficients of the J -dependent terms can be determined. A total of 766 CDs were obtained from the fundamental bands of which two thirds were from torsionally split lines. Originally CDs of each symmetry species were fit separately to determine if there were any dependence of the rotational constants on

symmetry or the corresponding nuclear spin. No statistically significant differences were found so all CDs were then fit simultaneously, resulting in the ground state constants given in table 1.

TABLE 1: Ground State Constants of $^{12}\text{C}_2\text{H}_6$ in cm^{-1}

A_o	$= 2.671^{(a)}$
B_o	$= 0.6630271(14)^{(b)}$
D_o^K	$= 1.09 \times 10^{-5}^{(c)}$
D_o^K	$= 2.660(29) \times 10^{-6}^{(b)}$
D_o^J	$= 1.0312(26) \times 10^{-6}^{(b)}$

^aRaman value for Ref. [26].

^bPresent work with uncertainties in parentheses representing one standard deviation.

^cCalculated value from Ref. [22].

Not only does the combination difference fitting provide an excellent set of rotational constants, but it also reflects the measurement precision obtained in this experiment. The standard deviation of the fit is 0.00055 cm^{-1} or 16.5 MHz . Since the ground state fitting is performed on differences, the measurement uncertainty of an individual line is reduced by a factor of $1/\sqrt{2}$ to $\sim 12 \text{ MHz}$. These ground state constants, given with near microwave precision, are certainly an improvement over prior lower resolution grating spectra determinations, and they are compatible with ultra precise Fourier transform interferometer data on ν_9 currently being analyzed [11].

5. Spectrum and Listing

We present in figure 6² the complete Doppler-limited absorption spectrum of ethane from 3051 cm^{-1} to 2870

cm^{-1} recorded at $T \approx 119 \text{ K}$. Prominent Q branches are labelled for ν_7 , and the $K = 0$ subband lines for the P(J) and R(J) manifolds are labelled for ν_5 . A listing of the measured transitions is given in table 2 consisting of the line center wavenumber, the peak intensity, the upper and lower state rotational quantum numbers when assigned, the ground state vibration-rotational-torsion symmetry in the G_{36}^+ group [21] when resolved (the subscript s is suppressed), the vibrational band code and the lower state energy. The vibrational band code is A for ν_7 , B for $\nu_8 + \nu_{11}$, C for ν_5 , and D for perturbation-induced lines. The lower state energy in wavenumbers is calculated from eq (1) using the precise rotational constants of table 1 and the more approximate values for A_o and D_o^K obtained from Raman spectra [26]. These ground state functions [3], are needed to compute the temperature dependence of the line intensities.

The intensity scale for figure 6 is given in $(\text{Torr} - \text{m})^{-1}$ taken from the “raw” experimental fill pressure at room temperature and the cell length. However, the experiment was conducted at constant density since the cell was sealed when the temperature was lowered. Thus for the listing of table 2 we convert the peak intensity units to $(\text{Amagat-cm})^{-1}$ by multiplying $(\text{Torr} - \text{m})^{-1}$ by the factor $(760/100) \times (295/273)/a = 8.397$ where $a = 0.978$ is the isotopic abundance of $^{12}\text{C}_2\text{H}_6$.

The authors are grateful to A. Mooradian and P. M. Moulton of MIT Lincoln Laboratory for the loan of the cold cell. They are also indebted to J. T. Hougen for numerous helpful discussions on the torsional symmetry and interactions in ethane.

²Figure 6 and table 2 are displayed on pages 244-256. References are on page 256.

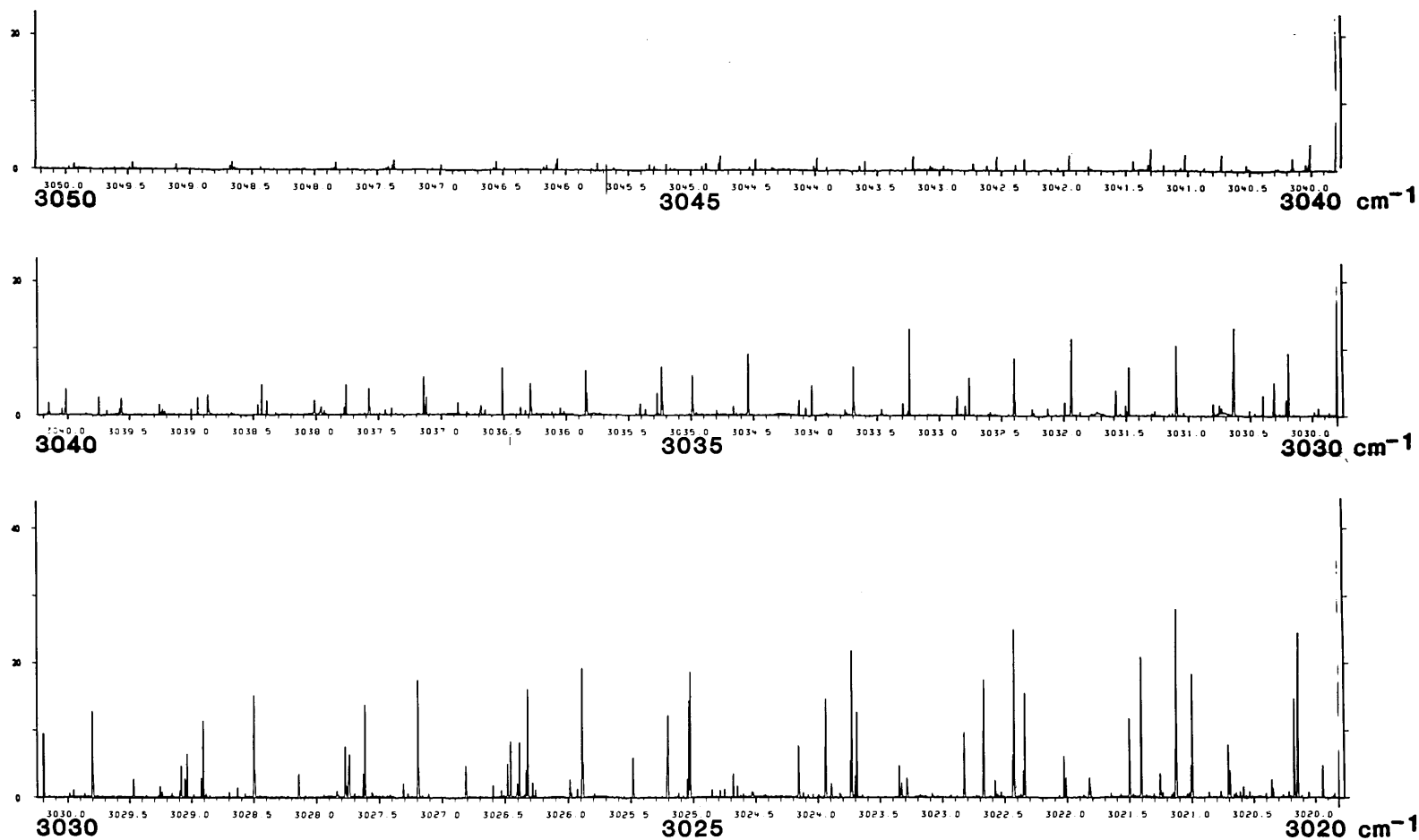


FIGURE 6. Doppler-limited spectrum of ethane at $T = 119$ K. The intensity scale is in $(\text{Torr}\cdot\text{m})^{-1}$ uncorrected for temperature or isotopes (see text).

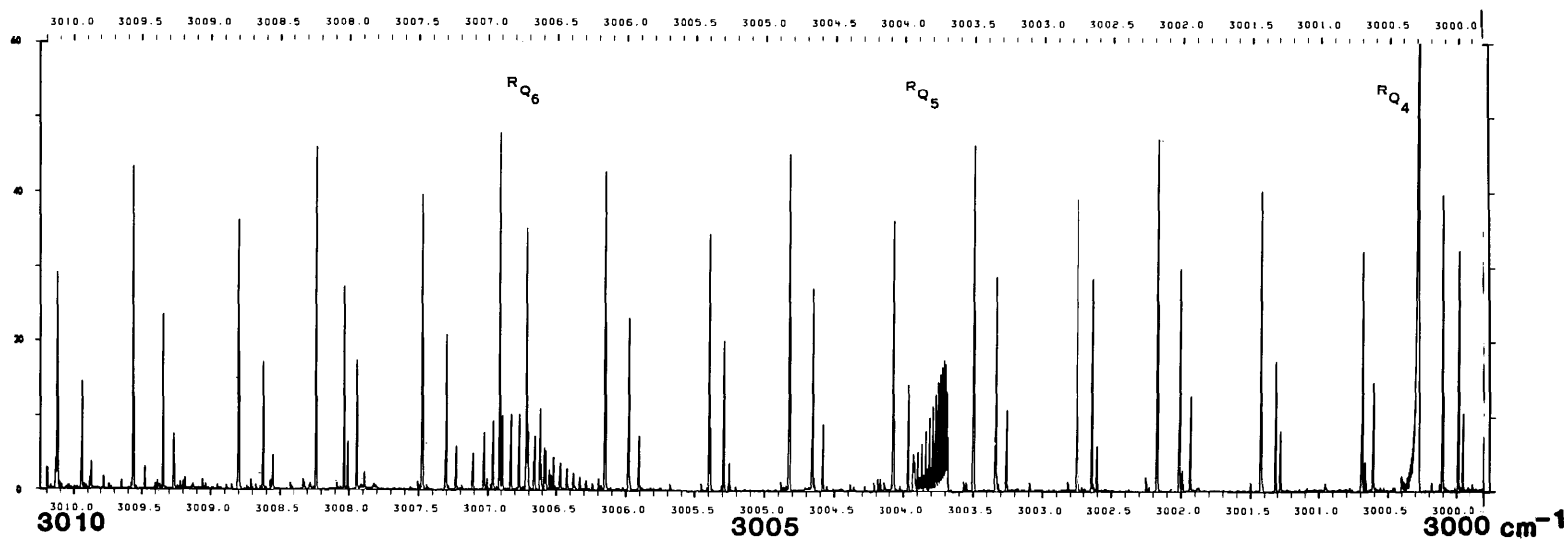
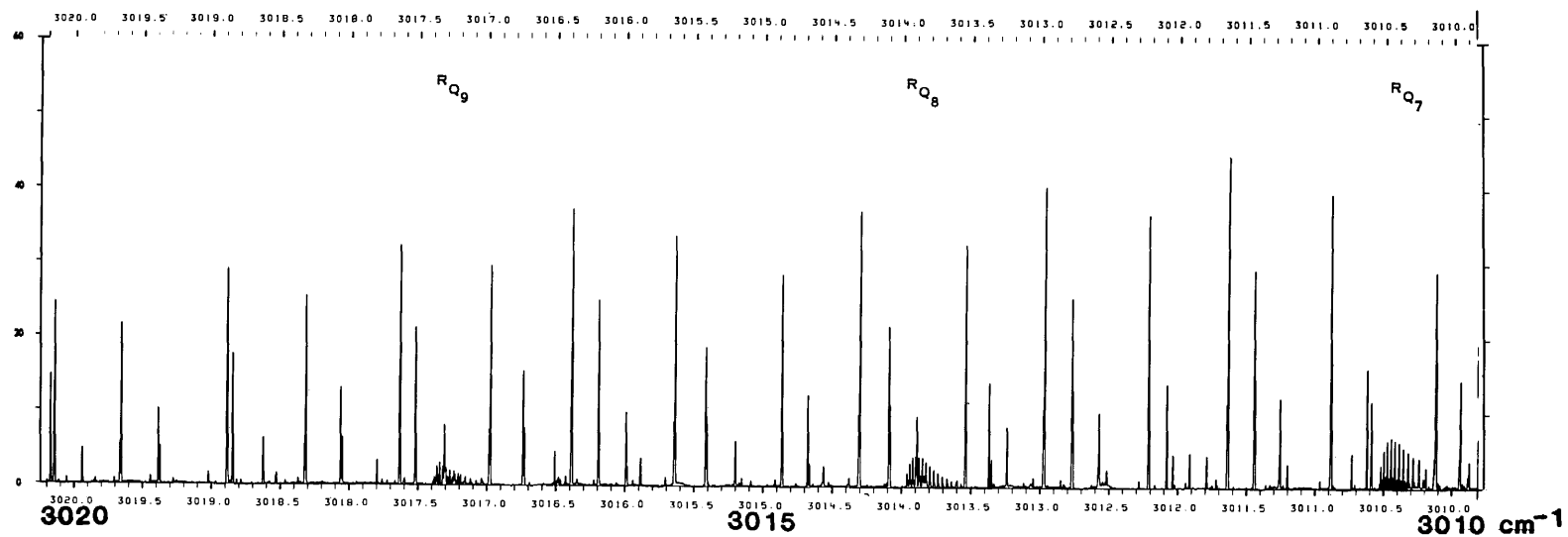


FIGURE 6. Continued

INTENSITY

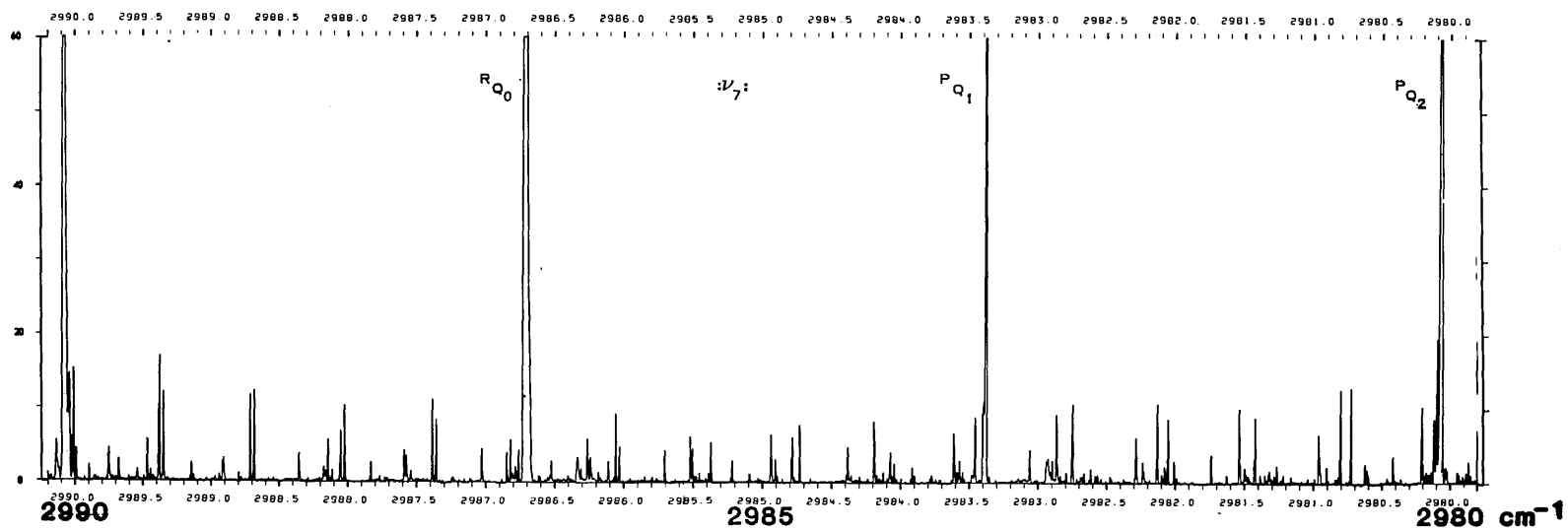
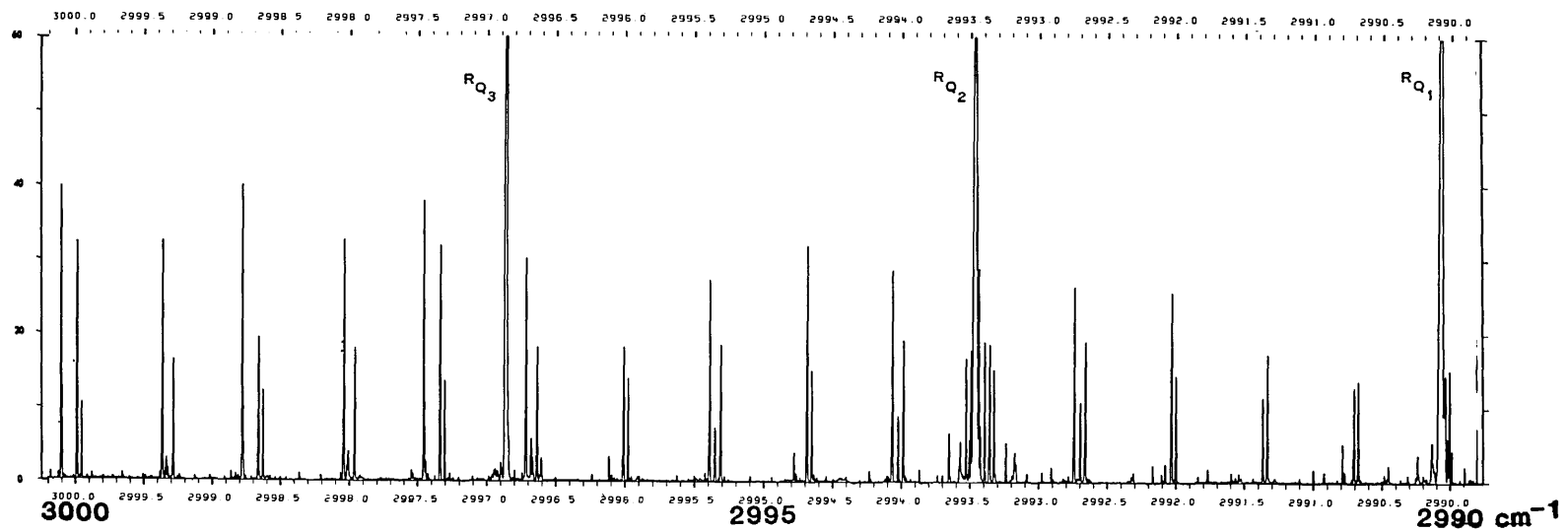


FIGURE 6. Continued

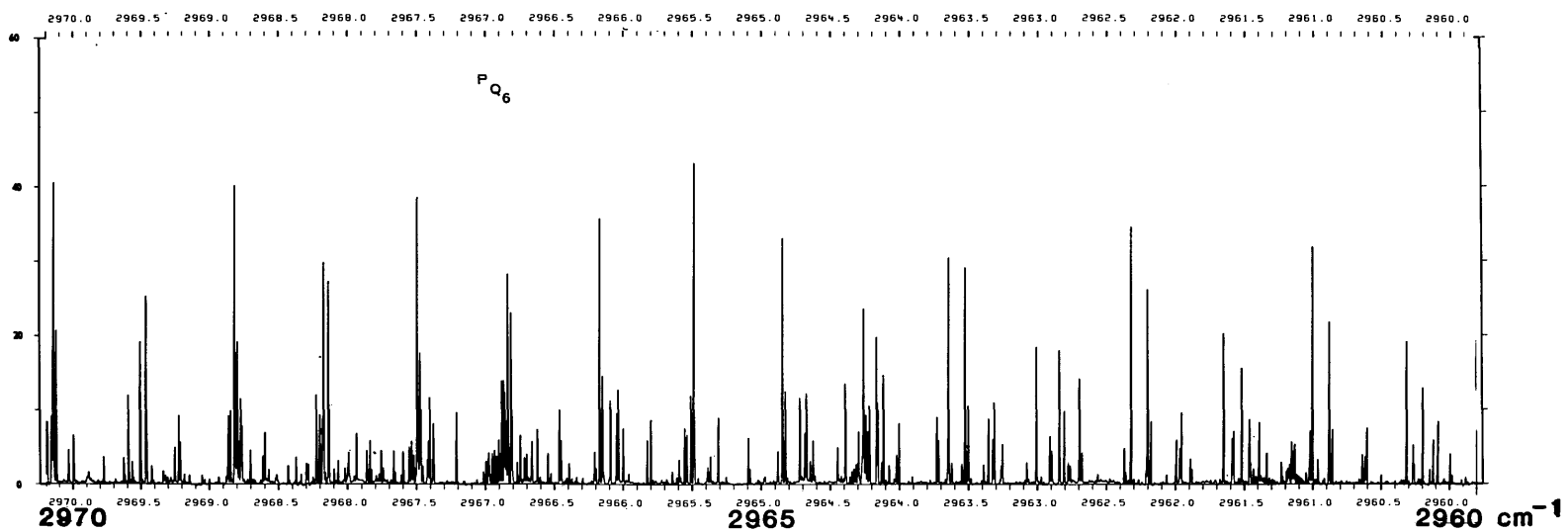
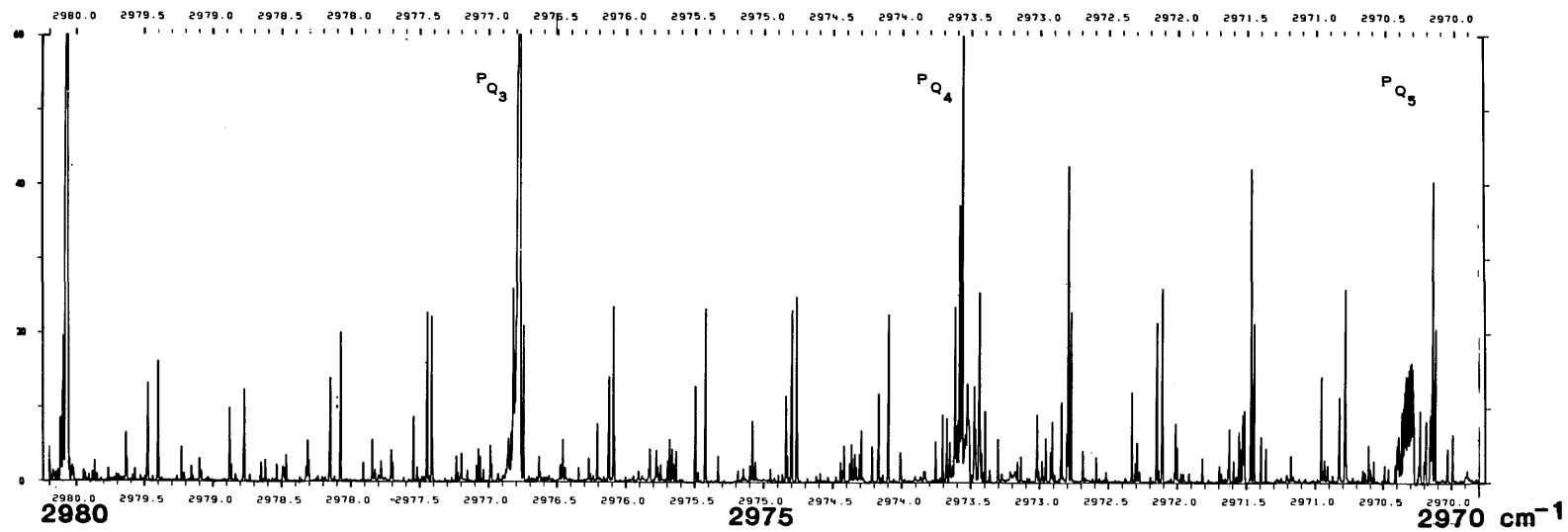


FIGURE 6. Continued

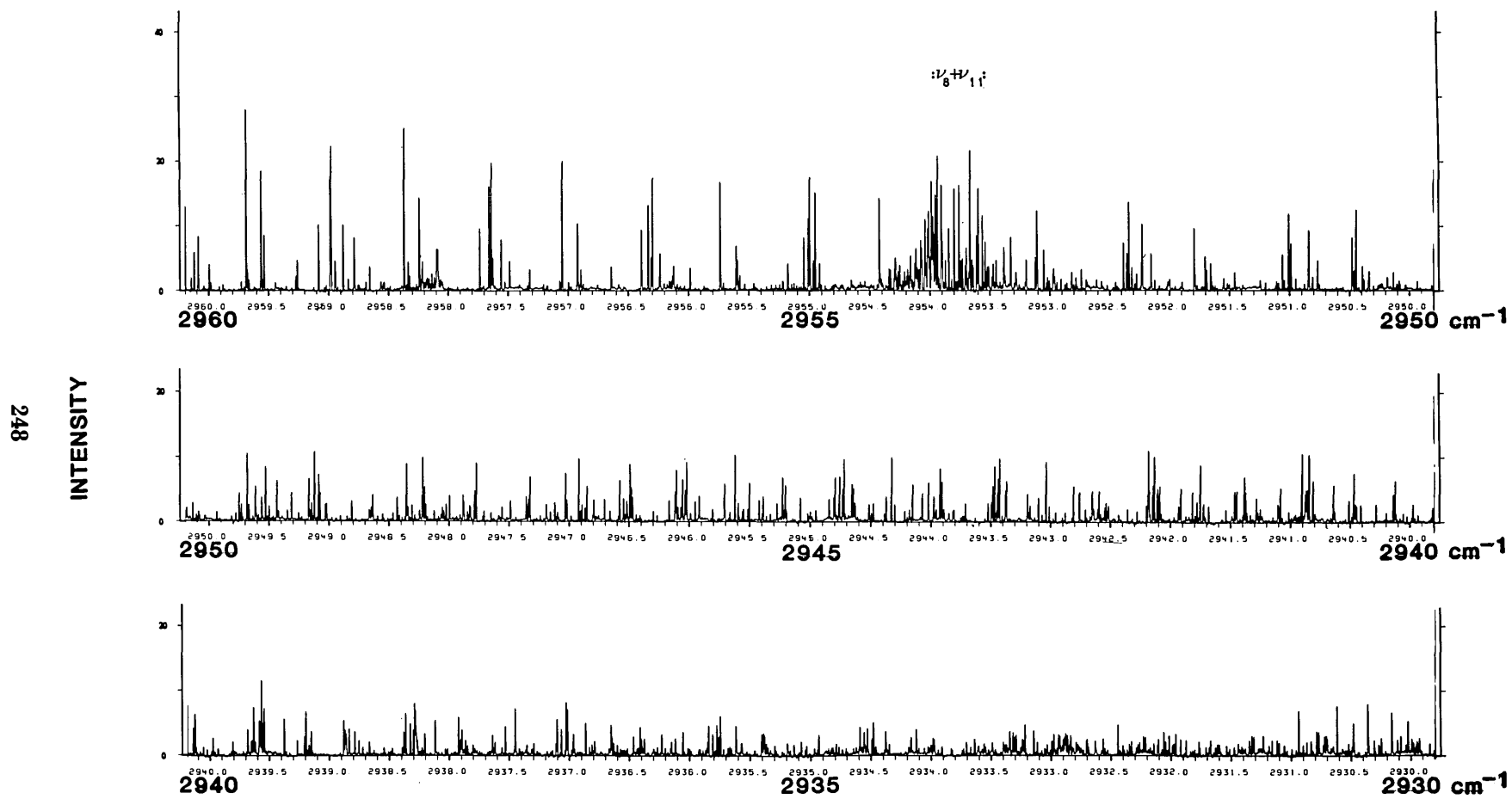


FIGURE 6. Continued

INTENSITY

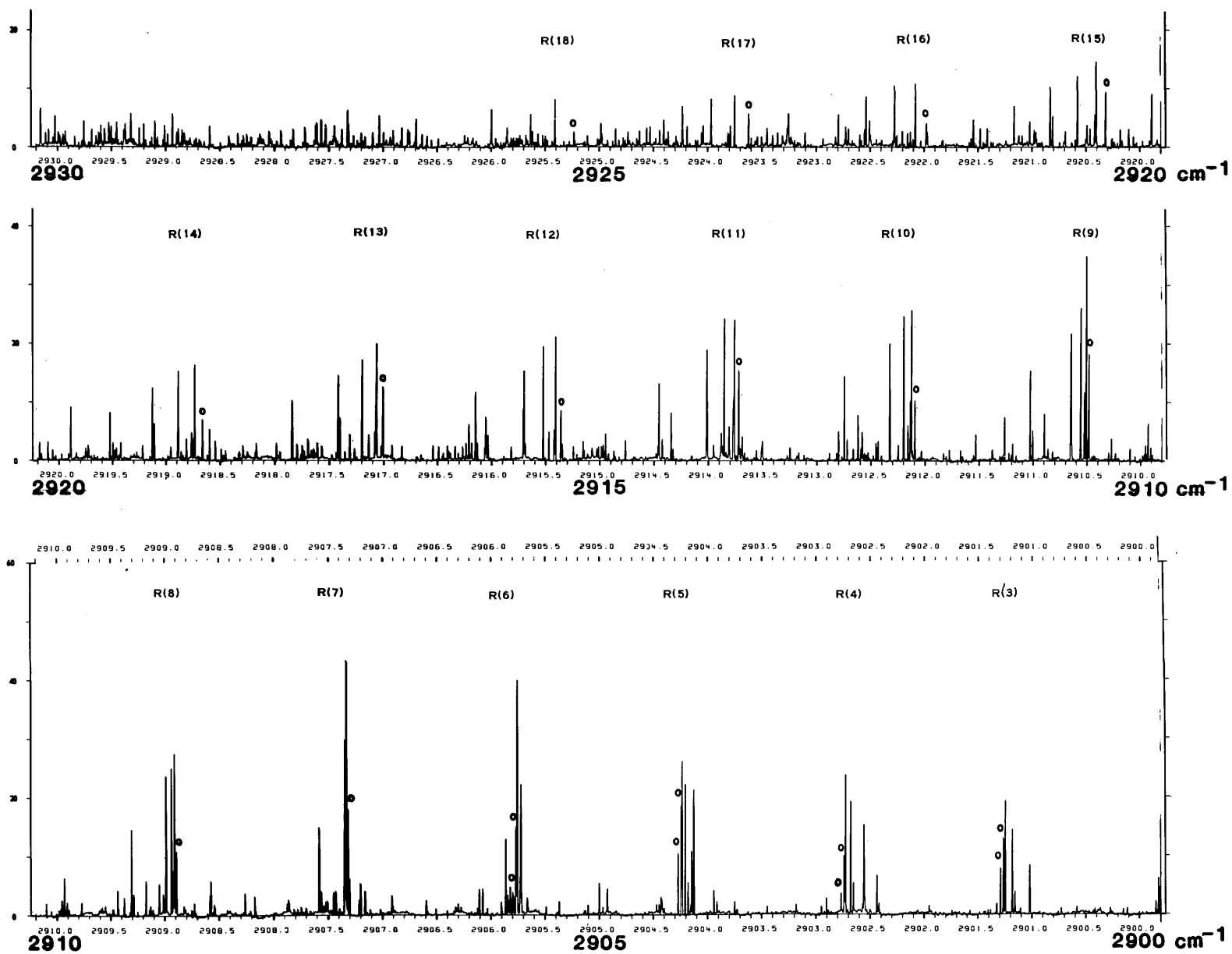


FIGURE 6. Continued

250

INTENSITY

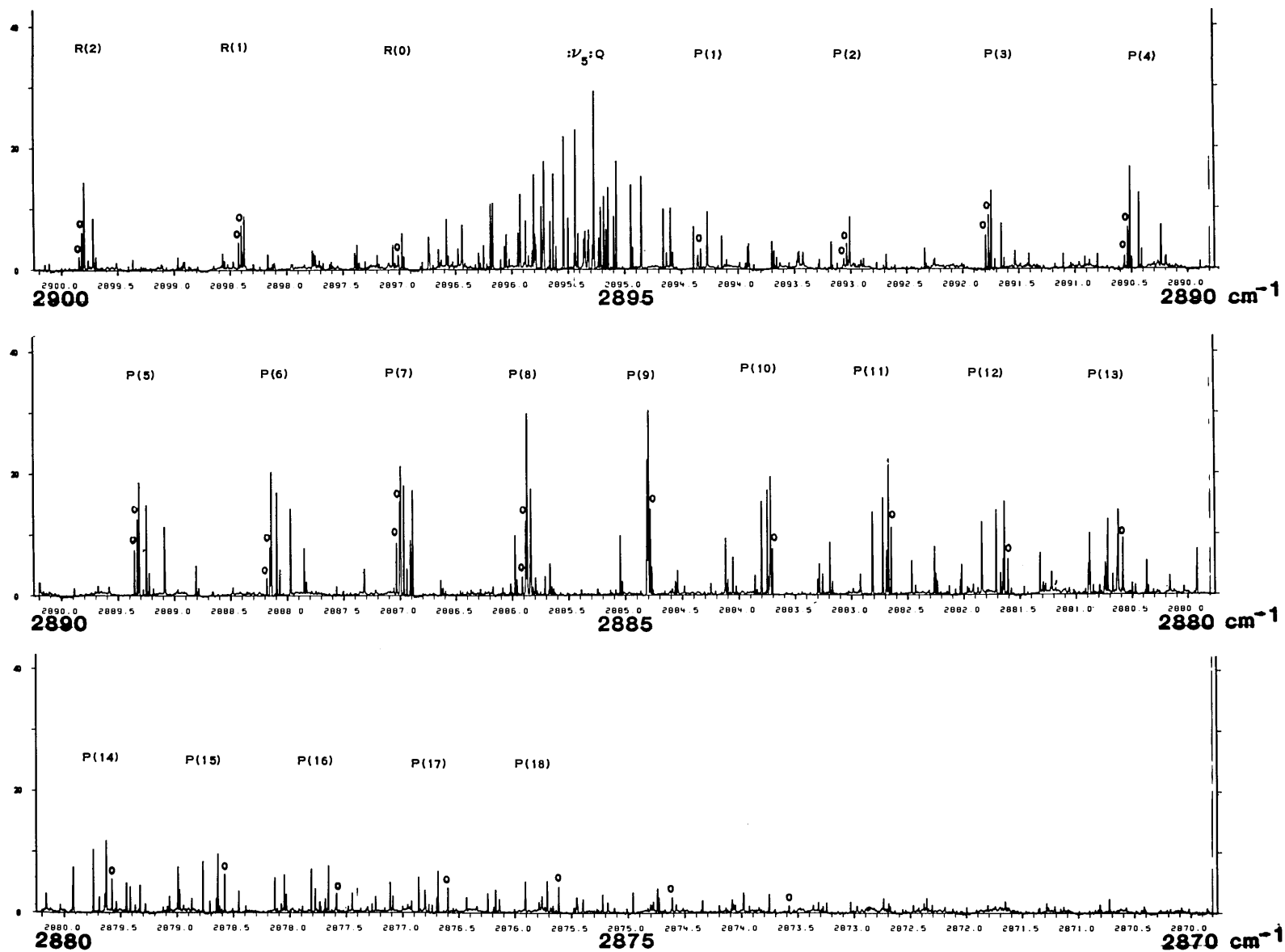


FIGURE 6. Continued

TABLE 2

TABLE 2. continued

WAVELENGTH (nm)	INT	TRANSITION J U JU JL JL	SYN BAND (nm)	E LOWER (nm)	WAVELENGTH (nm)	INT	TRANSITION J U JU JL JL	SYN BAND (nm)	E LOWER (nm)	WAVELENGTH (nm)	INT	TRANSITION J U JU JL JL	SYN BAND (nm)	E LOWER (nm)	WAVELENGTH (nm)	INT	TRANSITION J U JU JL JL	SYN BAND (nm)	E LOWER (nm)	WAVELENGTH (nm)	INT	TRANSITION J U JU JL JL	SYN BAND (nm)	E LOWER (nm)	
2993.1653	21.5				2989.4671	47.5	12 3 11 4 G	A	130.204	2986.0578	78.2	7 2 6 3			2982.8383	8.5				2980.1384	13.1				
2993.0852	9.9	7 4 8 3	A	114.490	2989.4683	12.9	12 3 11 4 E1	A	130.204	2986.0303	40.4	2 0 1 1			2982.7955	11.8				2980.1203	72.5				
2993.0752	11.8				2989.3844	18.5	2 1 1 0 E4	A	130.204	2986.0351	13.7	5 3 6 2 G	A	130.204	2982.7551	7.5	2 1 3 0 E4	A	7.956	2980.1083	46.7	1 1 2 2 G	A	14.662	
2993.0707	17.7	17 4 16 5 G	A	246.908	2989.3782	140.7	2 1 1 0 A2	A	130.204	2986.0312	51.7	5 3 6 2 G	A	130.204	2982.7489	88.8	2 1 3 0 A2	A	7.956	2980.0978	161.8	4 1 5 07 A2	A	19.888	
2993.0696	4.5	17 4 16 5 E1	A	246.908	2989.3504	101.5	7 1 6 2 G	A	130.204	2986.0305	13.7	5 3 6 2 E1	A	130.204	2982.6899	5.5	11 5 10 37 E3,4	B	302.036	2980.0928	26.3				
2993.0739	231.1	2 2 1 1	A	3.997	2989.3510	5.9	10 6 11 5 E1	A	134.238	2986.0306	39.2	9 3 8 4	A	90.456	2982.6836	10.4	2 1 3 0 A2,4	B	302.036	2980.0848	18.3				
2993.0663	91.4	12 2 1 1	A	126.417	2989.3423	19.9	10 6 11 5 G	A	134.238	2986.0307	10.6	2 1 3 0 A2,4	B	90.456	2982.6773	3.7	15 6 16 5 E1	A	246.908	2980.0835	16.9				
2993.0594	160.2	7 0 6 1	A	30.513	2989.3269	6.9	15 8 16 7	A	130.948	2986.0308	15.5	15 6 16 5 G	A	246.908	2982.6555	12.5	15 6 16 5 G	A	246.908	2980.0828	12.7				
2993.0594	160.2	7 0 6 1	A	30.513	2989.3157	23.3				2986.0309	46.4			2982.6460	8.5				2980.0818	19.0	17 3 16 3 E3,4	B	204.182		
2993.1492	18.8				2989.3066	27.0	14 4 13 5	A	187.346	2986.0310	8.2	13 6 14 5 E1	A	205.881	2982.6461	8.5				2980.0815	29.7	17 3 16 3 E3,4	B	204.182	
2993.1041	9.4	14 3 13 4 E1	A	165.313	2989.2974	9.5				2986.0311	28.3	13 6 14 5 E1	A	205.881	2982.6461	8.5				2980.0815	29.7	17 3 16 3 E3,4	B	204.182	
2993.0779	20.4	14 3 13 4 G	A	165.313	2989.2923	91.9	9 2 8 3	A	71.762	2986.0312	28.3	13 6 14 5 E1	A	205.881	2982.6461	8.5				2980.0815	29.7	17 3 16 3 E3,4	B	204.182	
2993.0366	175.3	4 1 3 0 E4	A	7.956	2989.2834	103.1	4 0 3 1	A	10.427	2986.0313	90.5	8 4 9 3 A1,2	A	85.688	2982.6461	8.5				2980.0815	29.7	17 3 16 3 E3,4	B	204.182	
2993.0310	211.9	4 1 3 0 A2	A	7.956	2989.2530	30.5	8 5 9 4	A	21.963	2986.0314	91.9	9 2 8 3	A	85.688	2982.6461	8.5				2980.0815	29.7	17 3 16 3 E3,4	B	204.182	
2993.0006	121.5	1 1 8 2	A	18.408	2989.2345	17.4	3 2 2 1	A	102.387	2986.0315	91.9	9 2 8 3	A	85.688	2982.6461	8.5				2980.0815	29.7	17 3 16 3 E3,4	B	204.182	
2993.0358	1.8	13 8 16 7 E1	A	269.961	2989.2389	12.7	11 3 10 47 E1	A	115.432	2986.0316	91.9	9 2 8 3	A	85.688	2982.6461	8.5				2980.0815	29.7	17 3 16 3 E3,4	B	204.182	
2993.0371	7.4	12 8 16 7 G	A	269.961	2989.2333	146.3	11 3 10 4 G	A	115.432	2986.0317	91.9	9 2 8 3	A	85.688	2982.6461	8.5				2980.0815	29.7	17 3 16 3 E3,4	B	204.182	
2993.0371	4.2	8 6 9 5 E1	A	126.417	2989.2338	13.9				2986.0318	91.9	9 2 8 3	A	85.688	2982.6461	8.5				2980.0815	29.7	17 3 16 3 E3,4	B	204.182	
2993.0371	15.4	8 6 9 5 G	A	126.417	2989.2338	13.9				2986.0319	91.9	9 2 8 3	A	85.688	2982.6461	8.5				2980.0815	29.7	17 3 16 3 E3,4	B	204.182	
2993.0371	15.4	8 6 9 5 G	A	126.417	2989.2338	13.9				2986.0320	91.9	9 2 8 3	A	85.688	2982.6461	8.5				2980.0815	29.7	17 3 16 3 E3,4	B	204.182	
2993.0371	15.4	8 6 9 5 G	A	126.417	2989.2338	13.9				2986.0321	91.9	9 2 8 3	A	85.688	2982.6461	8.5				2980.0815	29.7	17 3 16 3 E3,4	B	204.182	
2993.0371	15.4	8 6 9 5 G	A	126.417	2989.2338	13.9				2986.0322	91.9	9 2 8 3	A	85.688	2982.6461	8.5				2980.0815	29.7	17 3 16 3 E3,4	B	204.182	
2993.0371	15.4	8 6 9 5 G	A	126.417	2989.2338	13.9				2986.0323	91.9	9 2 8 3	A	85.688	2982.6461	8.5				2980.0815	29.7	17 3 16 3 E3,4	B	204.182	
2993.0371	15.4	8 6 9 5 G	A	126.417	2989.2338	13.9				2986.0324	91.9	9 2 8 3	A	85.688	2982.6461	8.5				2980.0815	29.7	17 3 16 3 E3,4	B	204.182	
2993.0371	15.4	8 6 9 5 G	A	126.417	2989.2338	13.9				2986.0325	91.9	9 2 8 3	A	85.688	2982.6461	8.5				2980.0815	29.7	17 3 16 3 E3,4	B	204.182	
2993.0371	15.4	8 6 9 5 G	A	126.417	2989.2338	13.9				2986.0326	91.9	9 2 8 3	A	85.688	2982.6461	8.5				2980.0815	29.7	17 3 16 3 E3,4	B	204.182	
2993.0371	15.4	8 6 9 5 G	A	126.417	2989.2338	13.9				2986.0327	91.9	9 2 8 3	A	85.688	2982.6461	8.5				2980.0815	29.7	17 3 16 3 E3,4	B	204.182	
2993.0371	15.4	8 6 9 5 G	A	126.417	2989.2338	13.9				2986.0328	91.9	9 2 8 3	A	85.688	2982.6461	8.5				2980.0815	29.7	17 3 16 3 E3,4	B	204.182	
2993.0371	15.4	8 6 9 5 G	A	126.417	2989.2338	13.9				2986.0329	91.9	9 2 8 3	A	85.688	2982.6461	8.5				2980.0815	29.7	17 3 16 3 E3,4	B	204.182	
2993.0371	15.4	8 6 9 5 G	A	126.417	2989.2338	13.9				2986.0330	91.9	9 2 8 3	A	85.688	2982.6461	8.5				2980.0815	29.7	17 3 16 3 E3,4	B	204.182	
2993.0371	15.4	8 6 9 5 G	A	126.417	2989.2338	13.9				2986.0331	91.9	9 2 8 3	A	85.688	2982.6461	8.5				2980.0815	29.7	17 3 16 3 E3,4	B	204.182	
2993.0371	15.4	8 6 9 5 G	A	126.417	2989.2338	13.9				2986.0332	91.9	9 2 8 3	A	85.688	2982.6461	8.5				2980.0815	29.7	17 3 16 3 E3,4	B	204.182	
2993.0371	15.4	8 6 9 5 G	A	126.417	2989.2338	13.9				2986.0333	91.9	9 2 8 3	A	85.688	2982.6461	8.5				2980.0815	29.7	17 3 16 3 E3,4	B	204.182	
2993.0371	15.4	8 6 9 5 G	A	126.417	2989.2338	13.9				2986.0334	91.9	9 2 8 3	A	85.688	2982.6461	8.5				2980.0815	29.7	17 3 16 3 E3,4	B	204.182	
2993.0371	15.4	8 6 9 5 G	A	126.417	2989.2338	13.9				2986.0335	91.9	9 2 8 3	A	85.688	2982.6461	8.5				2980.0815	29.7	17 3 16 3 E3,4	B	204.182	
2993.0371	15.4	8 6 9 5 G	A	126.417	2989.2338	13.9				2986.0336	91.9	9 2 8 3	A	85.688	2982.6461	8.5				2980.0815	29.7	17 3 16 3 E3,4	B	204.182	
2993.0371	15.4	8 6 9 5 G	A	126.417	2989.2338	13.9				2986.0337	91.9	9 2 8 3	A	85.688	2982.6461	8.5				2980.0815	29.7	17 3 16 3 E3,4	B	204.182	
2993.0371	15.4	8 6 9 5 G	A	126.417	2989.2338	13.9				2986.0338	91.9	9 2 8 3	A	85.688	2982.6461	8.5				2980.0815	29.7	17 3 16 3 E3,4	B	204.182	
2993.0371	15.4	8 6 9 5 G	A	126.417	2989.2338	13.9				2986.0339	91.9	9 2 8 3	A	85.688	2982.6461	8.5				2980.0815	29.7	17 3 16 3 E3,4	B	204.182	
2993.0371	15.4	8 6 9 5 G	A	126.417	2989.2338	13.9				2986.0340	91.9	9 2 8 3	A	85.688	2982.6461	8.5				2980.0815	29.7	17 3 16 3 E3,4	B	204.182	
2993.0371	15.4	8 6 9 5 G	A	126.417	2989.2338	13.9				2986.0341	91.9	9 2 8 3	A	85.688	2982.6461	8.5				2980.0815	29.7	17 3 16 3 E3,4	B	204.182	
2993.0371	15.4	8 6 9 5 G	A	126.417	2989.2338	13.9				2986.0342	91.9	9 2 8 3	A	85.688	2982.6461	8.5				2980.0815	29.7	17 3 16 3 E3,4	B	204.182	
2993.0371	15.4	8 6 9 5 G	A	126.417	2989.2338	13.9				2986.0343	91.9	9 2 8 3	A	85.688	2982.6461	8.5				2980.0815	29.7	17 3 16 3 E3,4	B	204.182	
2993.0371	15.4	8 6 9 5 G	A	126.417	2989.2338	13.9				2986.0344	91.9	9 2 8 3	A	85.688	2982.6461	8.5				2980.0815	29.7	17 3 16 3 E3,4	B	204.182	
2993.0371	15.4	8 6 9 5 G	A	126.417	2989.2338	13.9				2986.0345	91.9	9 2 8 3	A	85.688	2982.6461	8.5				2980.0815	29.7	17 3 16 3 E3,4	B	204.182	
2993.0371	15.4	8 6 9 5 G	A	126.417	2989.2338	13.9				2986.0346	91.9	9 2 8 3	A	85.688	2982.6461	8.5				2980.0815	29.7	17 3 16 3 E3,4	B	204.182	
2993.0371	15.4	8 6 9 5 G	A	126.417	2989.2338	13.9				2986.0347	91.9	9 2 8 3	A	85.688	2982.6461	8.5				2980.0815	29.7	17 3 16 3 E3,4	B	204.182	
2993.0371	15.4	8 6 9 5 G	A	126.417	2989.2338	13.9				2986.0348	91.9	9 2 8 3	A	85.688	2982.6461	8.5				2980.0815	29.7	17 3 16 3 E3,4	B	204.182	
2993.0371	15.4	8 6 9 5 G	A	126.417	2989.2338	13.9				2986.0349	91.9	9 2 8 3	A	85.688	2982.6461	8.5				2980.0815	29.7	17 3 16 3 E3,4	B	204.182	
2993.0371	15.4	8 6 9 5 G	A	126.417	2989.2338	13.9				2986.0350	91.9	9 2 8 3	A	85.688	2982.6461	8.5				2980.0815	29.7	17 3 16 3 E3,4</			

TABLE 2. continued

WAVELENGTH (nm)	INT	TRANSITION J U K L	STN BAND (nm)	E LOWER (nm)	WAVELENGTH (nm)	INT	TRANSITION J U K L	STN BAND (nm)	E LOWER (nm)	WAVELENGTH (nm)	INT	TRANSITION J U K L	STN BAND (nm)	E LOWER (nm)	WAVELENGTH (nm)	INT	TRANSITION J U K L	STN BAND (nm)	E LOWER (nm)	WAVELENGTH (nm)	INT	TRANSITION J U K L	STN BAND (nm)	E LOWER (nm)	
255.195	23.3				255.191	73.5				255.192	73.5				255.193	73.5				255.194	73.5				
255.196	133.5				255.197	13.2				255.198	13.2				255.199	13.2				255.200	13.2				
255.197	21.3				255.201	10.0				255.202	10.0				255.203	10.0				255.204	10.0				
255.201	32.2	9 1 8 1	B	50.395	255.205	4.4	5 3	B	47.800	255.206	75.6	6 0 5 0 A2	B	19.888	255.207	255.5	4 4 5 3	B	46.556	255.208	25.3				
255.202	46.7	8 2 7 2	B	47.800	255.209	10.2				255.210	10.2				255.211	10.2				255.212	10.2				
255.203	8.5				255.213	27.5				255.214	27.5				255.215	27.5				255.216	27.5				
255.206	75.6	6 0 5 0 A2	B	19.888	255.217	11.4				255.218	11.4				255.219	11.4				255.220	11.4				
255.207	49.6	6 0 5 0 A2	B	19.888	255.221	16.6				255.222	16.6				255.223	16.6				255.224	16.6				
255.208	255.5	4 4 5 3	B	46.556	255.225	24.1	2 10 3	A	96.738	255.226	24.1	2 10 3	A	96.738	255.227	24.1	2 10 3	A	96.738	255.228	24.1	2 10 3	A	96.738	
255.209	10.2				255.229	22.3				255.230	22.3				255.231	22.3				255.232	22.3				
255.210	10.2				255.233	24.1	2 10 3	A	96.738	255.234	24.1	2 10 3	A	96.738	255.235	24.1	2 10 3	A	96.738	255.236	24.1	2 10 3	A	96.738	
255.211	10.2				255.237	27.5				255.238	27.5				255.239	27.5				255.240	27.5				
255.212	10.2				255.241	11.4				255.242	11.4				255.243	11.4				255.244	11.4				
255.213	10.2				255.245	16.6				255.246	16.6				255.247	16.6				255.248	16.6				
255.214	10.2				255.249	22.3				255.250	22.3				255.251	22.3				255.252	22.3				
255.215	10.2				255.253	24.1	2 10 3	A	96.738	255.254	24.1	2 10 3	A	96.738	255.255	24.1	2 10 3	A	96.738	255.256	24.1	2 10 3	A	96.738	
255.216	10.2				255.257	27.5				255.258	27.5				255.259	27.5				255.260	27.5				
255.217	10.2				255.261	11.4				255.262	11.4				255.263	11.4				255.264	11.4				
255.218	10.2				255.265	16.6				255.266	16.6				255.267	16.6				255.268	16.6				
255.219	10.2				255.269	22.3				255.270	22.3				255.271	22.3				255.272	22.3				
255.220	10.2				255.273	24.1	2 10 3	A	96.738	255.274	24.1	2 10 3	A	96.738	255.275	24.1	2 10 3	A	96.738	255.276	24.1	2 10 3	A	96.738	
255.221	10.2				255.277	27.5				255.278	27.5				255.279	27.5				255.280	27.5				
255.222	10.2				255.281	11.4				255.282	11.4				255.283	11.4				255.284	11.4				
255.223	10.2				255.285	16.6				255.286	16.6				255.287	16.6				255.288	16.6				
255.224	10.2				255.289	22.3				255.290	22.3				255.291	22.3				255.292	22.3				
255.225	10.2				255.293	24.1	2 10 3	A	96.738	255.294	24.1	2 10 3	A	96.738	255.295	24.1	2 10 3	A	96.738	255.296	24.1	2 10 3	A	96.738	
255.226	10.2				255.297	27.5				255.298	27.5				255.299	27.5				255.300	27.5				
255.227	10.2				255.301	11.4				255.302	11.4				255.303	11.4				255.304	11.4				
255.228	10.2				255.305	16.6				255.306	16.6				255.307	16.6				255.308	16.6				
255.229	10.2				255.309	22.3				255.310	22.3				255.311	22.3				255.312	22.3				
255.230	10.2				255.313	24.1	2 10 3	A	96.738	255.314	24.1	2 10 3	A	96.738	255.315	24.1	2 10 3	A	96.738	255.316	24.1	2 10 3	A	96.738	
255.231	10.2				255.317	27.5				255.318	27.5				255.319	27.5				255.320	27.5				
255.232	10.2				255.321	11.4				255.322	11.4				255.323	11.4				255.324	11.4				
255.233	10.2				255.325	16.6				255.326	16.6				255.327	16.6				255.328	16.6				
255.234	10.2				255.329	22.3				255.330	22.3				255.331	22.3				255.332	22.3				
255.235	10.2				255.333	24.1	2 10 3	A	96.738	255.334	24.1	2 10 3	A	96.738	255.335	24.1	2 10 3	A	96.738	255.336	24.1	2 10 3	A	96.738	
255.236	10.2				255.337	27.5				255.338	27.5				255.339	27.5				255.340	27.5				
255.237	10.2				255.341	11.4				255.342	11.4				255.343	11.4				255.344	11.4				
255.238	10.2				255.345	16.6				255.346	16.6				255.347	16.6				255.348	16.6				
255.239	10.2				255.349	22.3				255.350	22.3				255.351	22.3				255.352	22.3				
255.240	10.2				255.353	24.1	2 10 3	A	96.738	255.354	24.1	2 10 3	A	96.738	255.355	24.1	2 10 3	A	96.738	255.356	24.1	2 10 3	A	96.738	
255.241	10.2				255.357	27.5				255.358	27.5				255.359	27.5				255.360	27.5				
255.242	10.2				255.361	11.4				255.362	11.4				255.363	11.4				255.364	11.4				
255.243	10.2				255.365	16.6				255.366	16.6				255.367	16.6				255.368	16.6				
255.244	10.2				255.369	22.3				255.370	22.3				255.371	22.3				255.372	22.3				
255.245	10.2				255.373	24.1	2 10 3	A	96.738	255.374	24.1	2 10 3	A	96.738	255.375	24.1	2 10 3	A	96.738	255.376	24.1	2 10 3	A	96.738	
255.246	10.2				255.377	27.5				255.378	27.5				255.379	27.5				255.380	27.5				
255.247	10.2				255.381	11.4				255.382	11.4				255.383	11.4				255.384	11.4				
255.248	10.2				255.385	16.6				255.386	16.6				255.387	16.6				255.388	16.6				
255.249	10.2				255.389	22.3				255.390	22.3				255.391	22.3				255.392	22.3				
255.250	10.2				255.393	24.1	2 10 3	A	96.738	255.394	24.1	2 10 3	A	96.738	255.395	24.1	2 10 3	A	96.738	255.396	24.1	2 10 3	A	96.738	
255.251	10.2				255.397	27.5				255.398	27.5				255.399	27.5				255.400	27.5				
255.252	10.2				255.401	11.4				255.402	11.4				255.403	11.4				255.404	11.4				
255.253	10.2				255.405	16.6				255.406	16.6				255.407	16.6				255.408	16.6				
255.254	10.2				255.409	22.3				255.410	22.3				255.411	22.3				255.412	22.3				
255.255	10.2				255.413	24.1	2 10 3	A	96.738	255.414	24.1	2 10 3	A	96.738	255.415	24.1	2 10 3	A	96.738	255.416	24.1	2 10 3	A	96.738	
255.256	10.2				255.417	27.5				255.418	27.5				255.419	27.5				255.420	27.5				
255.257	10.2				255.421	11.4				255.422	11.4				255.423	11.4				255.424	11.4				
255.258	10.2				255.425	16.6				255.426	16.6				255.427	16.6				255.428	16.6				
255.259	10.2				255.429	22.3				255.430	22.3				255.431	22.3				255.432	22.3				
255.260	10.2				255.433	24.1	2 10 3	A	96.738	255.434	24.1	2 10 3	A	96.738	255.435	24.1	2 10 3	A	96.738	255.436	24.1	2 10 3	A	96.738	
255.261	10.2				255.437	27.5				255.438	27.5				255.439	27.5				255.440	27.5				
255.262	10.2				255.441	11.4				255.442	11.4				255.443	11.4				255.444	11.4				
255.263	10.2				255.445	16.6				255.446	16.6				255.447	16.6				255.448	16.6				

TABLE 2. continued

WAVELENGTH (CH-1)	INT	TRANSITION J U R V J L KL	STH BAND	E LOWER (CH-1)	WAVELENGTH (CH-1)	INT	TRANSITION J U R V J L KL	STH BAND	E LOWER (CH-1)	WAVELENGTH (CH-1)	INT	TRANSITION J U R V J L KL	STH BAND	E LOWER (CH-1)	WAVELENGTH (CH-1)	INT	TRANSITION J U R V J L KL	STH BAND	E LOWER (CH-1)	WAVELENGTH (CH-1)	INT	TRANSITION J U R V J L KL	STH BAND	E LOWER (CH-1)	
2918.3005	33.0	11 3 12 3 E3,4	B	127.404	2918.3757	22.1				2918.4414	11.8				2918.4641	26.5				2918.4641	18.1				
2918.2813	47.7	11 3 12 3 A1,2	B	127.404	2918.3452	11.1				2918.3752	11.1				2918.4641	18.1				2918.4641	18.1				
2918.2815	14.3				2918.2806	27.7	11 1 12 1	B	104.038	2918.3455	14.6				2918.4124	25.9				2918.4124	25.9				
2918.2762	29.2				2918.2764	11.1				2918.3455	14.6				2918.4124	25.9				2918.4124	25.9				
2918.2644	19.7				2918.1582	9.5				2918.3455	14.6				2918.4124	25.9				2918.4124	25.9				
2918.2374	10.4				2918.1511	17.9				2918.3455	14.6				2918.4124	25.9				2918.4124	25.9				
2918.2043	28.3	14 2 15 2	B	169.456	2918.1817	22.3	12 2 13 2	B	131.246	2918.3455	14.6				2918.4124	25.9				2918.4124	25.9				
2918.1174	45.0	11 6 12 6	B	199.504	2918.0557	30.8				2918.3455	14.6				2918.4124	25.9				2918.4124	25.9				
2918.0142	8.7				2918.0159	9.2				2918.3455	14.6				2918.4124	25.9				2918.4124	25.9				
2917.9232	49.6	13 1 14 1	B	141.789	2918.0103	8.5				2918.3455	14.6				2918.4124	25.9				2918.4124	25.9				
2917.9046	20.7				2918.0103	8.5				2918.3455	14.6				2918.4124	25.9				2918.4124	25.9				
2917.8947	33.0				2918.0103	8.5				2918.3455	14.6				2918.4124	25.9				2918.4124	25.9				
2917.8647	19.1				2918.0103	8.5				2918.3455	14.6				2918.4124	25.9				2918.4124	25.9				
2917.8478	12.6				2918.0103	8.5				2918.3455	14.6				2918.4124	25.9				2918.4124	25.9				
2917.8022	13.4				2918.0103	8.5				2918.3455	14.6				2918.4124	25.9				2918.4124	25.9				
2917.7874	9.4				2918.0103	8.5				2918.3455	14.6				2918.4124	25.9				2918.4124	25.9				
2917.6476	9.9				2918.0103	8.5				2918.3455	14.6				2918.4124	25.9				2918.4124	25.9				
2917.6402	29.0	13 0 14 0 A1	B	139.118	2918.0103	8.5				2918.3455	14.6				2918.4124	25.9				2918.4124	25.9				
2917.6281	11.3	13 0 14 0 E3	B	139.118	2918.0103	8.5				2918.3455	14.6				2918.4124	25.9				2918.4124	25.9				
2917.6196	17.8				2918.0103	8.5				2918.3455	14.6				2918.4124	25.9				2918.4124	25.9				
2917.5844	10.6				2918.0103	8.5				2918.3455	14.6				2918.4124	25.9				2918.4124	25.9				
2917.5328	40.1	10 1 11 1	B	104.144	2918.0103	8.5				2918.3455	14.6				2918.4124	25.9				2918.4124	25.9				
2917.4507	40.4	11 2 12 21	B	114.051	2918.0103	8.5				2918.3455	14.6				2918.4124	25.9				2918.4124	25.9				
2917.4173	10.7				2918.0103	8.5				2918.3455	14.6				2918.4124	25.9				2918.4124	25.9				
2917.3524	13.1				2918.0103	8.5				2918.3455	14.6				2918.4124	25.9				2918.4124	25.9				
2917.2982	14.4				2918.0103	8.5				2918.3455	14.6				2918.4124	25.9				2918.4124	25.9				
2917.1862	8.4				2918.0103	8.5				2918.3455	14.6				2918.4124	25.9				2918.4124	25.9				
2917.1314	15.9				2918.0103	8.5				2918.3455	14.6				2918.4124	25.9				2918.4124	25.9				
2917.1012	47.1	12 4 13 4	B	163.313	2918.0103	8.5				2918.3455	14.6				2918.4124	25.9				2918.4124	25.9				
2917.0470	34.2				2918.0103	8.5				2918.3455	14.6				2918.4124	25.9				2918.4124	25.9				
2917.0255	48.8				2918.0103	8.5				2918.3455	14.6				2918.4124	25.9				2918.4124	25.9				
2917.0148	40.0				2918.0103	8.5				2918.3455	14.6				2918.4124	25.9				2918.4124	25.9				
2916.9647	10.4				2918.0103	8.5				2918.3455	14.6				2918.4124	25.9				2918.4124	25.9				
2916.9573	8.5				2918.0103	8.5				2918.3455	14.6				2918.4124	25.9				2918.4124	25.9				
2916.8834	42.0	12 6 13 6	B	216.718	2918.0103	8.5				2918.3455	14.6				2918.4124	25.9				2918.4124	25.9				
2916.8320	11.1	15 2 16 2	B	107.878	2918.0103	8.5				2918.3455	14.6				2918.4124	25.9				2918.4124	25.9				
2916.8114	14.2				2918.0103	8.5				2918.3455	14.6				2918.4124	25.9				2918.4124	25.9				
2916.7887	18.6				2918.0103	8.5				2918.3455	14.6				2918.4124	25.9				2918.4124	25.9				
2916.6700	9.2				2918.0103	8.5				2918.3455	14.6				2918.4124	25.9				2918.4124	25.9				
2916.6522	39.5	14 1 15 1	B	161.444	2918.0103	8.5				2918.3455	14.6				2918.4124	25.9				2918.4124	25.9				
2916.6453	24.0				2918.0103	8.5				2918.3455	14.6				2918.4124	25.9				2918.4124	25.9				
2916.6317	18.9				2918.0103	8.5				2918.3455	14.6				2918.4124	25.9				2918.4124	25.9				
2916.6014	16.2				2918.0103	8.5				2918.3455	14.6				2918.4124	25.9				2918.4124	25.9				
2916.5746	8.9				2918.0103	8.5				2918.3455	14.6				2918.4124	25.9				2918.4124	25.9				
2916.5552	9.7				2918.0103	8.5				2918.3455	14.6				2918.4124	25.9				2918.4124	25.9				
2916.4654	25.1				2918.0103	8.5				2918.3455	14.6				2918.4124	25.9				2918.4124	25.9				
2916.4353	9.2				2918.0103	8.5				2918.3455	14.6				2918.4124	25.9				2918.4124	25.9				
2916.4248	10.2				2918.0103	8.5				2918.3455	14.6				2918.4124	25.9				2918.4124	25.9				
2916.4123	37.2	14 0 15 0 A2	B	158.973	2918.0103	8.5				2918.3455	14.6				2918.4124	25.9				2918.4124	25.9				
2916.4000	22.1	14 0 15 0 E4	B	158.973	2918.0103	8.5				2918.3455	14.6				2918.4124	25.9				2918.4124	25.9				
2916.3865	19.9				2918.0103	8.5				2918.3455	14.6				2918.4124	25.9				2918.4124	25.9				
2916.3363	23.3				2918.0103	8.5				2918.3455	14.6				2918.4124	25.9				2918.4124	25.9				
2916.3000	15.1				2918.0103	8.5				2918.3455	14.6				2918.4124	25.9				2918.4124	25.9				
2916.2817	22.9				2918.0103	8.5				2918.3455	14.6				2918.4124	25.9				2918.4124	25.9				
2916.2544	22.3				2918.0103	8.5				2918.3455	14.6				2918.4124	25.9				2918.4124	25.9				
2916.2360	10.4				2918.0103	8.5				2918.3455	14.6				2918.4124	25.9				2918.4124	25.9				
2916.2289	11.1				2918.0103	8.5				2918.3455	14.6				2918.4124	25.9				2918.4124	25.9				
2916.2129	14.4				2918.0103	8.5				2918.3455	14.6				2918.4124	25.9				2918.4124	25.9				
2916.1486	8.9				2918.0103	8.5				2918.3455	14.6				2918.4124	25.9				2918.4124	25.9				
2916.1325	18.6				2918.0103	8.5				2918.3455	14.6				2918.4124	25.9				2918.4124	25.9				
2916.1231	10.2				2918.0103	8.5				2918.3455	14.6				2918.4124	25.9				2918.4124	25.9				
2916.1119	12.1				2918.0103	8.5				2918.3455	14.6				2918.4124	25.9				2918.4124	25.9				
2916.1031	10.8				2918.0103	8.5				2918.3455	14.6				2918.4124	25.9				2918.4124	25.9				
2916.0901	22.8				2918.0103	8.5				2918.3455	14.6				2918.4124	25.9				2918.4124	25.9				

TABLE 2. continued

(CH-1)	IPT	TRANSIT	STN BAND	E LOWER (CH-1)	WAVELENGTH (CH-1)	IPT	TRANSIT	STN BAND	E LOWER (CH-1)	WAVELENGTH (CH-1)	IPT	TRANSIT	STN BAND	E LOWER (CH-1)	WAVELENGTH (CH-1)	IPT	TRANSIT	STN BAND	E LOWER (CH-1)	WAVELENGTH (CH-1)	IPT	TRANSIT	STN BAND	E LOWER (CH-1)	WAVELENGTH (CH-1)	
2015-0747	17.8				2012-6288	26.5				2009-3233	6.1	12	5	11	81	C	150-336			2002-5975	21.1					
2015-0884	12.2				2012-6358	18.7	11	3	10	3	C	94-938								2002-7617	13.5	12	4	10	4	
2015-0900	10.1				2012-6425	16.1				2009-3817	9.0									2002-7854	19.5	5	4	10	3	
2015-0937	20.1				2012-6506	20.7	1	1	10	2	C	83-884								2002-8068	16.1	5	2	4	2	
2015-0985	20.9				2012-6606	40.6	11	1	10	1	C	110-400								2002-8464	16.1	5	2	4	2	
2015-1000	10.1				2012-6685	15.1	11	1	10	1	C	75-572								2002-8672	15.1	5	2	4	2	
2015-1036	12.2				2012-6727	25.2	11	1	10	1	C	75-572								2002-8672	15.1	5	2	4	2	
2015-1062	10.2				2012-6866	38.5				2012-6866	38.5									2002-8672	15.1	5	2	4	2	
2015-1221	10.2				2012-6964	26.1	11	0	10	0	C	72-901								2002-8672	15.1	5	2	4	2	
2015-1236	10.2				2012-6985	18.7				2012-6985	18.7									2002-8672	15.1	5	2	4	2	
2015-1747	28.0				2011-8304	10.8				2008-9392	10.2	2	8	2	8	C	36-408			2001-7347	10.9					
2015-1849	20.0				2011-8407	21.3				2008-9392	10.2	2	8	2	8	C	36-408			2001-7347	10.9					
2015-1900	10.1				2011-8728	15.0	14	5	13	5	C	187-346								2001-7347	10.9					
2015-2043	10.0				2011-8823	15.1				2008-9392	10.2	2	8	2	8	C	36-408			2001-7347	10.9					
2015-2452	10.0	12	4	1	4	0	C	130-204												2001-7347	10.9					
2015-2500	10.1				2011-9307	15.1				2008-9392	10.2	2	8	2	8	C	36-408			2001-7347	10.9					
2015-2633	68.3	11	6	10	5	0	C	139-668												2001-7347	10.9					
2015-2656	11.0	11	0	10	1	0	C	139-668												2001-7347	10.9					
2015-3024	10.1				2011-9612	8.9				2008-9392	10.2	2	8	2	8	C	36-408			2001-7347	10.9					
2015-3162	10.0	12	3	11	3	1	C	111-510												2001-7347	10.9					
2015-3206	10.0	12	3	11	3	1	C	111-510												2001-7347	10.9					
2015-3226	18.8				2011-9612	8.9				2008-9392	10.2	2	8	2	8	C	36-408			2001-7347	10.9					
2015-3503	99.6	14	6	3	6	1	C	216-718												2001-7347	10.9					
2015-3526	10.0	12	3	11	3	1	C	111-510												2001-7347	10.9					
2015-3559	20.3	12	2	11	2	0	C	98-157												2001-7347	10.9					
2015-3665	12.1	12	2	11	2	1	C	98-157												2001-7347	10.9					
2015-3699	85.3	11	1	11	1	1	C	90-164												2001-7347	10.9					
2015-3722	13.2	12	0	11	0	0	C	87-473												2001-7347	10.9					
2015-3745	10.1				2012-6288	26.5				2009-3233	6.1	12	5	11	81	C	150-336			2002-5975	21.1					
2015-3768	10.1				2012-6358	18.7	11	3	10	3	C	94-938								2002-7617	13.5	12	4	10	4	
2015-3791	10.1				2012-6425	16.1				2009-3817	9.0									2002-7854	19.5	5	4	10	3	
2015-3814	10.1				2012-6506	20.7	1	1	10	2	C	83-884								2002-8068	16.1	5	2	4	2	
2015-3837	10.1				2012-6606	40.6	11	1	10	1	C	110-400								2002-8464	16.1	5	2	4	2	
2015-3860	10.1				2012-6685	15.1	11	1	10	1	C	75-572								2002-8672	15.1	5	2	4	2	
2015-3883	10.1				2012-6727	25.2	11	1	10	1	C	75-572								2002-8672	15.1	5	2	4	2	
2015-3906	10.1				2012-6866	38.5				2012-6866	38.5									2002-8672	15.1	5	2	4	2	
2015-3929	10.1				2012-6964	26.1	11	0	10	0	C	72-901								2002-8672	15.1	5	2	4	2	
2015-3952	10.1				2012-6985	18.7				2012-6985	18.7									2002-8672	15.1	5	2	4	2	
2015-3975	10.1				2011-8304	10.8				2008-9392	10.2	2	8	2	8	C	36-408			2001-7347	10.9					
2015-3998	10.1				2011-8407	21.3				2008-9392	10.2	2	8	2	8	C	36-408			2001-7347	10.9					
2015-4021	10.1				2011-8728	15.0	14	5	13	5	C	187-346								2001-7347	10.9					
2015-4044	10.1				2011-8823	15.1				2008-9392	10.2	2	8	2	8	C	36-408			2001-7347	10.9					
2015-4067	10.1				2011-9307	15.1				2008-9392	10.2	2	8	2	8	C	36-408			2001-7347	10.9					
2015-4090	10.1				2011-9612	8.9				2008-9392	10.2	2	8	2	8	C	36-408			2001-7347	10.9					
2015-4113	10.1				2011-9823	15.1				2008-9392	10.2	2	8	2	8	C	36-408			2001-7347	10.9					
2015-4136	10.1				2011-1004	15.1				2008-9392	10.2	2	8	2	8	C	36-408			2001-7347	10.9					
2015-4159	10.1				2011-1027	15.1				2008-9392	10.2	2	8	2	8	C	36-408			2001-7347	10.9					
2015-4182	10.1				2011-1050	15.1				2008-9392	10.2	2	8	2	8	C	36-408			2001-7347	10.9					
2015-4205	10.1				2011-1073	15.1				2008-9392	10.2	2	8	2	8	C	36-408			2001-7347	10.9					
2015-4228	10.1				2011-1096	15.1				2008-9392	10.2	2	8	2	8	C	36-408			2001-7347	10.9					
2015-4251	10.1				2011-1119	15.1				2008-9392	10.2	2	8	2	8	C	36-408			2001-7347	10.9					
2015-4274	10.1				2011-1142	15.1				2008-9392	10.2	2	8	2	8	C	36-408			2001-7347	10.9					
2015-4297	10.1				2011-1165	15.1				2008-9392	10.2	2	8	2	8	C	36-408			2001-7347	10.9					
2015-4320	10.1				2011-1188	15.1				2008-9392	10.2	2	8	2	8	C	36-408			2001-7347	10.9					
2015-4343	10.1				2011-1211	15.1				2008-9392	10.2	2	8	2	8	C	36-408			2001-7347	10.9					
2015-4366	10.1				2011-1234	15.1				2008-9392	10.2	2	8	2	8	C	36-408			2001-7347	10.9					
2015-4389	10.1				2011-1257	15.1				2008-9392	10.2	2	8	2	8	C	36-408			2001-7347	10.9					
2015-4412	10.1				2011-1280	15.1				2008-9392	10.2	2	8	2	8	C	36-408			2001-7347	10.9					
2015-4435	10.1				2011-1303	15.1				2008-9392	10.2	2	8	2	8	C	36-408			2001-7347	10.9					
2015-4458	10.1				2011-1326	15.1				2008-9392	10.2	2	8	2	8	C	36-408			2001-7347	10.9					
2015-4481	10.1				2011-1349	15.1				2008-9392	10.2	2	8	2	8	C	36-408			2001-7347	10.9					
2015-4504	10.1				2011-1372	15.1				2008-9392	10.2	2	8	2	8	C	36-408			2001-7347	10.9					
2015-4527	10.1				2011-1395	15.1				2008-9392	10.2	2	8	2	8	C	36-408			2001-7347	10.9					
2015-4550	10.1				2011-1418	15.1				2008-9392	10.2	2	8	2	8	C	36-408			2001-7347	10.9					
2015-4573	10.1				2011-1441	15.1				2008-9392	10.2	2	8	2	8	C	36-408			2001-7347	10.9					
2015-4596	10.1				2011-1464	15.1				2008-9392	10.2	2	8	2	8	C	36-408			2001-7347	10.9					
2015-4619	10.1				2011-1487	15.1				2008-9392	10.2	2	8	2	8	C	36-408			2001-734						

TABLE 2. continued

WAVELENGTH	INT.	TRANSITION	STN	BAUD	E	LOWER	WAVELENGTH	INT.	TRANSITION	STN	BAUD	E	LOWER
2875 7628	23 5						2875 2123	12 4					
2875 7370	9 2						2875 8086	11 8					
2875 7166	46 4	17 1 18 1	C	229	115		2875 7258	19 8	13 5 14 4	D	181	848	
2875 6660	10 2						2875 6183	9 0					
2875 6147	36 5	17 0 18 0	C	226	464		2869 8572	6 1	18 6 19 6 A1,2	C	347	694	
2875 6044	21 8	14 6 15 6 A1,2	C	255	106		2869 8607	2 2	18 6 19 6 E3,4	C	347	694	
2875 6478	12 1	14 6 15 6 E3,4	C	255	106		2869 5820	9 2					
2875 5910	19 2	18 6 19 6	C	294	293		2869 2293	11 4					
2875 5250	25 4	18 3 19 3 A1,2	C	275	601		2869 0962	15 2	14 5 15 4	D	201	703	
2875 1807	14 9	18 3 19 3 E3,4	C	275	601		2867 7530	9 7					
2874 9581	28 6	18 2 19 2	C	202	248		2867 6389	11 6					
2874 8036	11 9						2867 4641	14 9	15 5 16 4	D	222	875	
2874 7616	10 2						2866 5375	9 7					
2874 7602	15 9						2866 0385	10 9					
2874 7422	34 0	18 1 19 1	C	254	237		2865 8316	7 5	16 5 17 4	D	245	365	
2874 7288	21 8	13 5 14 5 C	C	205	881		2864 7715	9 7					
2874 6761	8 0	13 5 14 5 E1	C	205	881		2864 6353	14 4					
2874 6129	24 3	18 0 19 0	C	251	586		2864 4327	8 7					
2874 5785	12 9						2864 3029	8 7					
2874 3653	17 5	19 3 20 3 A1,2	C	302	036		2864 1960	12 2					
2874 1900	11 5	19 3 20 3 E3,4	C	302	036		2864 1133	9 7					
2874 0852	18 8	15 6 16 6 A1,2	C	276	278		2863 4629	9 9					
2874 0719	12 4	15 6 16 6 E3,4	C	276	278		2863 0441	8 5					
2874 0564	11 4						2863 0153	8 7					
2873 9876	28 1	11 5 12 4	D	146	098		2862 8202	9 9					
2873 9329	9 7												
2873 7563	26 1	18 1 20 1	C	280	673								
2873 5785	9 9	18 0 20 0	C	278	002								
2873 3648	10 9												
2873 3184	14 7												
2873 2785	8 9												
2873 2480	14 1	14 5 15 5	C	225	735								
2873 0337	15 4	20 2 21 2	C	318	433								
2872 9752	10 2												
2872 8855	8 4												
2872 8706	9 5												
2872 8576	8 7												
2872 7401	20 8	20 1 21 1	C	308	421								
2872 6940	13 9	16 6 17 6 A1,2	C	298	768								
2872 6816	9 7	16 6 17 6 E3,4	C	298	768								
2872 4767	11 4												
2872 3766	13 7												
2872 3561	20 9	12 5 13 4	D	183	313								
2872 1087	11 4												
2872 1955	8 5												
2871 8108	10 9	15 5 16 5	C	246	908								
2871 6506	16 4	21 1 22 1	C	317	483								
2871 2842	12 4	17 6 18 6 A1,2	C	322	573								
2871 2650	7 7	17 6 18 6 E3,4	C	322	573								
2871 2123	12 4												

6. References

- [1] Cole, A. R. H.; Lafferty, W. J.; Thibault, R. J. J. *Mol. Spectrosc.* **29**, 365-374 (1969).
- [2] Cole, A. R. H.; Cross, K. J.; Cugley, J. A.; Heise, H. M. J. *Mol. Spectrosc.* **83**, 233-244 (1980).
- [3] Herzberg, G. *Infrared and Raman Spectra of Polyatomic Molecules*, D. Van Nostrand Co., New York, 1959, Chapter IV and V.
- [4] Pitzer, K. S. *Dis. Faraday Soc.* **10**, 66-73 (1951).
- [5] Pitzer, R. M. *Accounts of Chem. Res.* in press.
- [6] Weiss, S.; Leroi, G. E. J. *Chem. Phys.* **48**, 962-967 (1967).
- [7] Hirota, E.; Saito, S.; Endo, Y. J. *Chem. Phys.*
- [8] Susskind, J. J. *Mol. Spectrosc.* **49**, 1-17 (1974).
- [9] Wilson, E. B. J. *Chem. Phys.* **6**, 740-745 (1938).
- [10] Patterson, C. W.; Flicker, H.; McDowell, R. S.; Nereson, N. *Mol. Phys.*
- [11] Lafferty, W. J.; Hougen, J. T.; Valentin, A.; Henry, L.; Malathy-Devi, V.; Das, P. P.; Rao, K. N. 36th Symposium on Molecular Spectroscopy, Paper WE2, Columbus, Ohio, June 1981.
- [12] Daunt, S. J.; Jennings, D. E.; Brault, J. W.; Susskind, J.; Reuter, D.; Blass, W. E. 36th Symposium on Molecular Spectroscopy, Paper WE3, Columbus, Ohio, June 1981.
- [13] Westcott, M. R. Alberta Research Council and Hinkley, E. D. Jet Propulsion Laboratory, private communication.
- [14] Toth, R. A. Jet Propulsion Laboratory, private communication.
- [15] Tokunaga, A. T.; Knacke, R. F.; Ridgway, S. T.; Wallace, L. *Astrophysical J.* **222**, 603-615 (1979).
- [16] Pine, A. S. J. *Opt. Soc. Amer.* **64**, 1683-1690 (1974).
- [17] Pine, A. S. J. *Opt. Soc. Amer.* **66**, 97-108 (1976).
- [18] Pine, A. S. in *Laser Spectroscopy III*, (J. L. Hall and J. T. Carlsten, Eds.), pp. 376-381, Springer-Verlag, New York, 1977.
- [19] Coulombe, M. J.; Pine, A. S. *Appl. Opt.* **18**, 1505-1512 (1979).
- [20] Tarrago, G.; Dang-Nhu, M.; Poussigue, G.; Guelachvili, G.; Amiot, C. J. *Mol. Spectrosc.* **57**, 246-263 (1975).
- [21] Hougen, J. T. *Can. J. Phys.* **42**, 1920-1937 (1964).
- [22] Nakagawa, I.; Shimanouchi, T. J. *Mol. Spectrosc.* **39**, 255-274 (1971).
- [23] Hougen, J. T. J. *Chem. Phys.* **38**, 1167-1173 (1963).
- [24] Olson, W. B., private communication.
- [25] Hougen, J. T. J. *Mol. Spectrosc.* **82**, 92-116 (1980).
- [26] Lepard, D. W.; Shaw, D. E.; Welsh, H. L. *Can. J. Phys.* **44**, 2353-2362 (1966).